Inhibition of Pitting Corrosion in 316L Stainless Steel: an evaluation of the phenomena *and* method to facilitate material selection for processing equipment

Emma Håkansson

MASTER THESIS, MATERIAL CHEMISTRY KASM10, 30 ECTS, 29th of May 2024

LTH
LUNDS TEKNISKA HÖGSKOLA

Supervisors:
Martin Adell (Technology Platform Manager, Tetra Pak)
Filip Lenrick (Senior Lecturer, Production and Materials Engineering)

Examiner:
Martin Ek Rosén (Senior Lecturer, Centre for Analysis and Synthesis)

Author:
Emma Håkansson

Lund University
Department of Chemistry
Centre for Analysis and Synthesis
P.O. Box 124
SE-221 00 Lund, Sweden

Abstract

This master's thesis is written for Tetra Pak with the aim to investigate if pitting corrosion inhibition can be detected for Stainless Steel 316L in contact with dairy products in an experimental setup. The aim was also to continue developing a corrosion test method to facilitate for material selection of food processing equipment in order to reduce the extent of detrimental pitting corrosion. The experimental work was conducted with the help of the department of Production and Materials Engineering at Lund University. A corrosion testing machine was utilized in order to follow the corrosion of the SS 316L samples. The corrosion testing routine was modified to suit food processing conditions with modifications to the sample preparation and the implementation of a cleaning in place (CIP) routine to combat fouling and biofilm-growth in the machine. Pitting corrosion of SS 316L was inhibited by the presence of dairy in the electrolyte for all assessed parameters except for the salt concentration 100 000 ppm (10wt%). The results can provide insight into the material selection of food processing equipment if compared to real-life pitting corrosion and industry knowledge. The method shows great promise to utilize in testing novel food products in which the industry lacks knowledge and make informed material choices of processing equipment. Necessary developments to further use the method is to eliminate crevice corrosion and alter the electrochemical measurements to suit the operating conditions.

Sammanfattning

Detta examensarbete är skrivet för Tetra Pak med syfte att undersöka huruvida mjölkprodukter experimentellt kan påvisas hämma gropfrätningskorrosion för det rostfria stålet 316L. Syftet var också att vidareutveckla en testmetod för korrosion som potentiellt kan underlätta i materialval till livsmedelsindustrin och således minska förekomsten av oönskad gropfrätningskorrosion i processutrustning. Rapportens experimentella del genomfördes med hjälp av institutionen för Industriell Produktion vid Lunds universitet. Den experimentella metoden anpassades bland annat för att fungera med livsmedel och med den ytsträvhet som är standard i livsmedelsindustin. Dessa anpassningar inkluderade bland annat en anpassning av provupparbetningen och implementering av kemisk rengöring för att förhindra kontaminering och biofilms-tillväxt i maskinen. En mjölkprodukt kunde påvisas hämma gropfrätningskorrosionen för rostfritt stål 316L vid alla testade parametrar förutom vid den högsta saltkoncentrationen. Resultaten som presenteras i denna rapport kan nyttjas för materialval om dessa jämförs med branschkunskap och riktiga fall av gropfrätningskorrosion. Metoden kan framgent till exempelvis användas för att testa korrosions motstånd av konstruktionsmaterial i kontakt med nya livsmedel som branschen saknar omfattande processkunskap om. Metoden bör vidareutvecklas så att spaltkorrosion elimnieras och anpassning av de elektrokemiska mätningarna bör göras för att passa driftsförhållanden.

Preface

This master thesis was written for Tetra Pak in Lund during the spring of 2024 with help of the department of Production and Materials Engineering at Lund University. The aim of this thesis was to contribute to Tetra Paks understanding of localized corrosion of stainless steel to aid in material selection of food processing equipment. I want to thank my supervisors Martin Adell and Filip Lenrick for their patience, help and enthusiasm during this project. I also want to thank everybody at the Production and Materials Engineering for their assistance and especially Mikael Hörndahl that always came up with solutions to fix anything and everything that leaked, broke or got stuck.

List of abbreviations, symbols and terms

CIP	Cleaning in place
CPDP	Cyclic potentiodynamic polarization
E_{corr}	Corrosion potential
E_{pit}	Pitting potential
E_{prot}	Protection potential
EDL	Electrical double layer
LIBS	Laser Induced Breakdown Spectroscopy
OCP	Open Circuit-potential
PMM	Population marginal mean
R_p	Polarization resistance
SHE	Standard Hydrogen Electrode
SMP	Skim Milk Powder
SMS	Simulated milk solution
SS	Stainless steel
XRF	X-ray Fluorescence

List of Figures

List of Tables

Contents

1 Introduction

The global food demand is expected to increase by 50% by the year 2050. To meet these demands while reducing the carbon footprint of food production requires improvements across the whole food supply chain [7]. Ongoing efforts to increase production efficiency while ensuring food safety and keeping the cost down includes optimization of food processing material selection. Stainless steels (SS) are often utilized due to their excellent corrosion resistance, ability to withstand both chemical and mechanical stress and ease of cleaning to comply with food safety requirements. However SSs can be subject to *pitting corrosion* which is a type of localized corrosion that is hard to predict and detrimental to the properties and service life of SS components. Choosing the correct stainless steel grade in accordance to food chemistry and processing parameters can mitigate or eliminate pitting corrosion and in turn reduce component replacement frequency. Selecting an insufficient SS grade will amount to a loss in money, resources and reduction in production efficiency [8]. Pitting corrosion is among other factors correlated to chloride concentration, temperature and the properties of the alloy [2] and has been reported to be inhibited in the presence of specific molecules [9]. Food chemistry is often complex and predicting which SS grade to use whilst not over-engineering components can be difficult as both (pitting corrosion) inducing and inhibiting effects can be present. A method to rapidly test materials for pitting corrosion during simulated processing has previously been developed by a master student in collaboration with Tetra Pak and the department of Production and Materials Engineering at Lund University [10]. The method is in this thesis utilized, evaluated and further developed to evaluate the inhibitory effect of dairy products on pitting corrosion in SS 316L during varying processing parameters and NaCl-concentrations. The results and development of method can set a foundation for comparison between experimental results and real-life pitting corrosion in equipment and could per example aid in material selection for processing novel food products where the industry lack experience.

1.1 Purpose and goal

The aim of this master's thesis is to evaluate the inhibitory effect on 316L stainless steel by dairy in food processing conditions. The aim is also to adjust and evaluate how the previously developed method [10] operates with dairy products to further utilize it in order to predict pitting corrosion of Tetra Paks food processing equipment.

1.2 Objectives

The objectives of this report was the following:

- Adjust the method to suit SS 316L for food processing standards, test how dairy products affects the pasteurizer and setup and develop a cleaning in place (CIP) routine.
- Test SS 316L samples according to a full factorial design for different temperatures, salt concentrations and dairy concentrations to evaluate the inhibitory effect of pitting corrosion.
- Conduct a literature review on the chemistry of pitting corrosion, how it can be measured, what can affect it and ultimately how it can be inhibited of SS 316L in dairy solutions.

1.3 Delimitations

The limit the scope of this thesis only one type of dairy product and stainless steel was assessed. The results are therefore specific the steel and dairy chemistry for the tested parameters. The pitting corrosion

was solely evaluated based on the electrochemical measurements and no extensive surface analysis of the samples was conducted. The main deliveries of the report is the i) evaluation of pitting parameters induced by variations of processing parameters by following a full-factorial design of experiment and ii) an evaluation of the test method for dairy products.

1.4 Structure of report

The report is structured into the following main sections containing:

- *Background (Section 2)* - A literature review of i) localized corrosion, how to measure it using the previously developed method and factors affecting the corrosion and method in terms of i) alloy composition ii) inhibitors and iii) dairy chemistry and processing.
- *Method and experimental design (Section 3)* - A description of the design of experiment, methods used to conduct the dynamic corrosion measurements and how the data was analyzed.
- *Results and discussion (Section 4)* - Results and suggested interpretations to utilize the data to aid in material selection of food processing equipment.
- *Conclusions & Outlook (Sections 5 and 6)* - Conclusions from the report is presented and future improvements to the method, analysis and testing is suggested.

2 Background

The following section describes the localized corrosion phenomena and its relevance for stainless steels in food processing applications, how it can be followed with electrochemical methods and factors affecting the risk of corrosion.

2.1 Corrosion and electrochemical reactions

Corrosion is a spontaneous deterioration process of metals caused by interactions with the environment. In a spontaneous process the product is thermodynamically favored, i.e the Gibbs free energy of the system decreases as the reaction proceeds to form products. The rate at which the reaction proceeds towards corrosion products is kinetically controlled and is accelerated at elevated temperatures and pressures [2]. Species that reacts to favor corrosion include acids, some halogens, water and oxygen. Products formed in corrosion reactions can be salts, carbonates, hydroxides and oxides [11]. General corrosion (also called uniform corrosion) is the most common type of corrosion. In general corrosion the electrochemical reactions proceed across an entire metal interface, with the anodic and cathodic sites constantly switching [12], see figure 1.

Stainless steels exhibit great resistance to general corrosion but is susceptible to pitting- and crevice corrosion, which are types of localized corrosion [13]. Localized corrosion attacks occurs on discrete sites, with fixed anodic and cathodic locations. Localized attacks occurs where protection by the passive oxide film fails. Prediction of localized corrosion is a challenge due to the small scale and the high rate of growth after pit initiation. Another challenge is that the chemistry and boundaries of the system is dynamic [14] and that *when* and *where* pitting is initiated is stochastically governed [15].

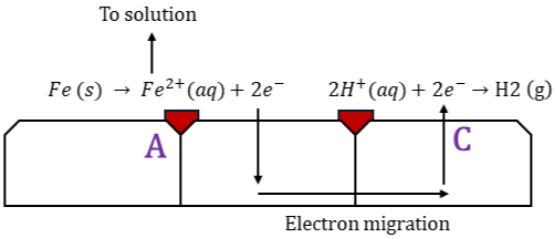

Figure 1: General corrosion of iron, A denotes anode and C denotes cathode. During uniform corrosion iron ions are dissolved. At anodic sites the red symbolize the corrosion product rust.

To understand corrosion electrochemistry, the study on how ions cross interfaces between electrolytes and solids, is required [16]. Electrochemical reactions are governed by differences in potential and exchange of electrons, which in turn can be described by thermodynamics and kinetics. The simplest form of an electrochemical cell consists of two conductive electrodes in contact with an electrolyte. The electrolyte conduct charge between the electrodes due to potential differences between the electrodes. Since solutions and/or salts can not conduct electrons, these are carried by ionic species. These react with the electrodes, resulting in an effective change of charge of both ions and electrodes to keep net neutrality. Cathodes accepts electrons in a reduction reactions and anodes donates electrons in a oxidation reaction [17]. In the above presented uniform corrosion (figure 1), it is for example during the anodic reaction metal loss occurs [1]. To follow the corrosion phenomena an external potential can be applied in both anodic and cathodic direction from the resting potential of the system. For example when an external potential in the anodic direction (increasing potential) is applied the anodic reactions are favored. This is described in more detail in section 2.2.2.

In the case of stainless steels a passive oxide layer protects the bulk metal limiting the electrical conductivity, which is presented further in section 2.4.2. Metals immersed in solutions also undergo

ionization (limited in presence of an passive oxide layer), resulting in an electrical double layer (EDL), see figure 2. The metal becomes partially negative which results in positive charges close to the surface of the metal. As these positive ions adsorb or associate close to the metal, a diffuse mobile layer of negative charges is attracted to the positive layer. The EDL is affected by the presence of salts in solution, external potential applied and by reactions taking place at the surface. For example, during a reduction the diffuse mobile layer moves closer to the positive layer, while during an oxidation the opposite occurs. A microscopically heterogeneous surface also results in variations across the electrical double layer. In summary, a passive oxide layer and the electrical double layer both make for a dynamic environment at the surface of a metal immersed in solution [17]. The EDL greatly affects the reactions at the surface, as all species included in corrosion reactions must pass the EDL [1].

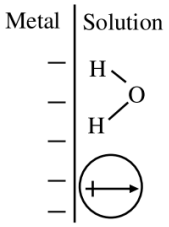

Figure 2: Electrical double layer (EDL) of metal immersed in water [1].

2.1.1 Pitting corrosion

Pitting corrosion is severe form of localized corrosion leading to the creation of small subsurface holes or *pits* on the metal surface. It can result in perforation of the metal and act as sites for stress-corrosion cracking during applied stress. The pits can be difficult to detect as they can be covered by corrosion products [1]. Pitting corrosion is governed by the composition and surface of the alloy, chloride concentration and acidity of electrolyte and temperature, among other factors. When performing an electrochemical measurement to test a materials pitting susceptibility, the potential applied and the scan rate (V/s) affect the propagation and onset of pitting corrosion. Localized damage to the passive oxide-layer, inclusions by impurities also contribute to an increased risk of pitting corrosion in alloys [2]. Pits can require long time to appear (years or months) and short term absence of pits does not indicate that a material is immune to pitting. Studies on preferential sites for pitting to occur indicate that a majority initiate and grow near scratched lines from for example mechanical polishing, as these cause strain hardening on the surface. In these zones the potential across the surface varies, resulting in increased risk of pitting at certain locations. Pits can also interact with each other, both increasing the rate of pitting and limiting the growth. During positive interaction the pits coalescence, which is often seen in service materials attacked by pitting corrosion [14]. Many metals has either an engineered or native passive oxide layer and in absence of aggressive anions, these can remain passive until the oxygen evolution potential. When measuring and applying an external potential it is important to keep below this potential. The passive layer is damaged in presence of anions, especially chlorides, which allow for pitting corrosion at lower potential than the oxygen evolution potential. The potential where this occurs and pitting is propagated is called the pitting potential, denoted E_{pit}. Pits can repassivate, depending on environment and on the site of the pit. Cathodic reactions occurring close can repassivate it, which is the same principle as when introducing cathodic current in a electrochemical measurement, allowing for a slower rate of propagation and growth [1]. Repassivation requires access to oxygen atoms to regenerate the oxide layer however increasing dissolved oxygen content in electrolytes is associated with an increased risk of

general corrosion [18].

Attempts has been made to create numerical models for pitting corrosion to predict the process. A few challenges in developing models has been the moving interface, shape and dimensions of pits and the presence of a dynamic electrical double layer. The ionic transport in the electrolyte is often not included in the model, however the ion transport is important in diffusion controlled electrochemical reactions, such as pitting corrosion [14].

Pitting can be initiated below the pitting potential, however these metastable pits are shortlived and usually repassivate within seconds [1]. They are initiated at preferential sites followed by almost immediate repassivation. Metastable pits are characterized by a sudden increase followed by a decrease of current density. They can repassivate since the critical conditions of acidity and presence of chloride ions are not met, which is required for stable pit growth. Chloride ions promote both nucleation and growth of metastable pits. A stable passive film, such as the chromium oxide in stainless steels, greatly reduce the preferred initiation sites for metastable pitting [19].

Pitting corrosion develops in three steps, i) initiation, by breakdown of the passive oxide film or by permeating it ii) growth of metastable pits, which can repassivate again and finally if they are not repassivated, iii) growth of stable and large pits. The first step starts with migration of chloride ions from the electrolyte to the passive oxide layer. The ions then permeate the passive layer, and interact with the bulk metal, however how the passive layer is permeated differs for different oxide layers [2]. The breakdown of the passive layer has been proposed to be by either penetration, adsorption or passive film breaking. All of which has been proposed for pure metals. One example of a reaction route where passive film breaking occurs is for iron in water, in which iron exhibits a hydrated passive layer which is converted into ferritic ions by the following reaction, see formula 1 below.

$$\mathrm{FeOOH} + \mathrm{H_2O} \longrightarrow \mathrm{Fe^{3+}} + 3\,\mathrm{OH^-} \tag{1}$$

In presence of chloride ions this reaction path is altered, by two coupled reactions, see eq 2 and 3. An intermediate compound, FeOCl, is created and deposited as islands on the passive film.

$$\mathrm{FeOOH} + \mathrm{Cl^-} \longrightarrow \mathrm{FeOCl} + \mathrm{OH^-} \tag{2}$$

$$\mathrm{FeOCl} + \mathrm{H_2O} \longrightarrow \mathrm{Fe^{3+}} + \mathrm{Cl^-} + 2\,\mathrm{OH^-} \tag{3}$$

The compound then reacts with water resulting in dissolved iron ions, chloride ions and hydroxide. At the sites of islands the passive film is removed and the underlying iron is subsequently dissolved into ferritic ions. The presence of chloride ions lower the activation energy to obtain passive film breakdown, as well as altering the reaction route. In short, increasing the chloride ions in the system decreases the potential (E_{pit}) required for the pitting reactions to be favored. Pit propagation is theorized to accelerate when the pit interior is acidified by a local presence of dissolved metal ions following the hydrolysis. The metal cation hydrolysis, see eq 4, results in a local pH decrease (net production of hydrogen ions) and a local chloride concentration increase (to keep the net neutrality when an excess of hydrogen ions are present) [2].

$$\mathrm{Fe^{2+}} + 2\,\mathrm{H_2O} \longrightarrow \mathrm{Fe(OH)_2} + 2\,\mathrm{H^+} \tag{4}$$

In summary, once a pit nucleates, pit propagation proceeds auto-catalytically [19]. See figure 3 for a schematic of the pitting process.

In stainless steels the breakdown of the passive layer occurs at preferential heterogeneous sites, such as sulphide inclusions [19] [20]. This and other factors governing localized corrosion in stainless steels

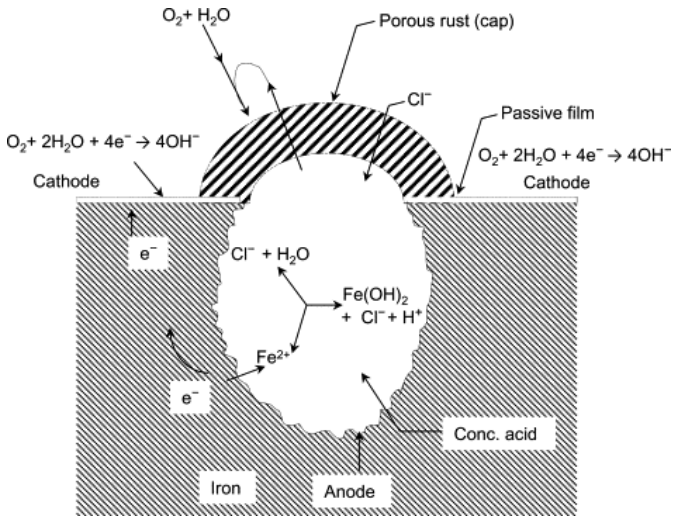

Figure 3: Pitting corrosion of iron [2].

is described in section 2.4.

2.1.2 Crevice corrosion

Crevice corrosion is a type of localized corrosion that occurs in crevices formed by stagnant flow of solution, especially common at welds, valves and in between gaskets and the metal [2]. Under deposit corrosion is a type of crevice corrosion in which an inert solid either is precipitated or deposited on the surface, allowing for a crevice to form in between at the interface of the inert solid and metal. Crevice corrosion can be characterized by a conjunction of general corrosion and pitting corrosion reactions [21]. The onset of crevice corrosion is usually at higher potentials compared to pitting corrosion and the current increase is not as rapid during corrosion measurements [2].

The chemistry in the crevice is often more aggressive compared to the bulk electrolyte. A few factors contribute to this, firstly the separation of anodic and cathodic sites leads to concentration differences, secondly the hydrolysis and metal cation dissolution (same as for pitting-corrosion) leads to a lower pH. The decrease of pH leads to a mass flux of chloride ions to the crevice to uphold the charge neutrality [22]. The cathodic and anodic reactions that initiate crevice corrosion can be seen in eq 5 and 6 [2]. The cathodic reaction occurs both on internal and external metallic surfaces [1].

$$O_2 + 2H_2O + 4e^- \longrightarrow 4OH^- \,(\text{reduction of oxygen}) \tag{5}$$

$$Fe \longrightarrow Fe^{2+} + 2e^- \,(\text{oxidation of iron}) \tag{6}$$

The limited mass transport of ferritic ions out of the crevice results in hydrolysis, increasing the acidity locally, same reaction route as for pitting.

$$Fe^{2+} + 2H_2O \longrightarrow Fe(OH)_2 + 2H^+ \,(\text{hydrolysis of iron}) \tag{7}$$

Crevice and pitting corrosion are both results of localized chemistry, with the difference between the two being that crevice corrosion requires a physically occluded site, where mass transport is limited [22]. An illustration of crevice corrosion can be found in figure 4.

Crevice corrosion proceeds in three stages, i) incubation, ii) propagation and iii) stifling. During

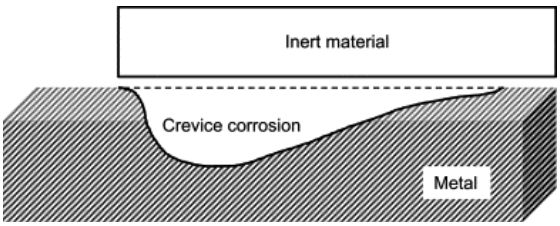

Figure 4: Illustration of crevice corrosion [2].

the incubation the local chemistry in the physical region is evolving towards the conditions required for propagation. Initially there is no difference in chemistry between the bulk electrolyte and the crevice, metal dissolution and oxygen reduction occur at similar rates accross the surface. However, the oxygen supply in the crevice is limited by diffusion which leads the previously mentioned separation of anodic and cathodic reactions. When oxygen is depleted, it becomes an anodic region. As the cathodic region (outside the crevice) is much larger than the anodic, this accelerates the dissolution in the crevice. This creates as mentioned, local acidification and a net flux of chloride ions to maintain net neutrality. If the rate of dissolution in the crevice is low and/or if it occurs so that the extent of physical occlusion decreases, the process of stifling begins. Dissolution is haltered, the pH increases locally and the surface can repassivate with the access of oxygen [22].

2.2 Measuring corrosion parameters

There are many ways to measure and follow corrosion. Electrochemical methods are often considered advantageous [23], as these are rapid and sensitive. Corrosion is dynamic process and involve a large number of parameters that are hard to control during measurement. To fully characterize a corrosion process it is common to employ a combination of methods. In the following section the techniques used in this report is presented.

2.2.1 Open circuit potential (OCP)

The open circuit potential (OCP) is the potential between the reference and working electrode in a system where the circuit is not closed, i.e bypassing the counter electrode. The OCP is indicative of the resting potential of a system, where the electrochemical reactions are at equilibrium, resulting in a zero current. OCP is also called Corrosion Potential (CP), since the sample will corrode at this potential, when the kinetics allow for it [24]. Corrosion Potential, also denoted E_{corr}, can be measured through potentiodynamic polarization and should be equal to the OCP, however this is not always the case [25], which is explained in section 2.2.2. According to Wagner and Traud, OCP/E_{corr}-potential is the steady-state potential, which lies between the two half-cell reactions and is a mixed potential. There is no net current however there is a small flux of metals from the metal surface [1]. The OCP is dependent on the passivisation layer and its' semiconducting ability. OCP can be measured for an extended period of time to determine stability of the system and to determine the starting point of a polarization measurement [26]. The stability and evolution of the OCP-value is highly dependent on the surface and the conditions during the oxide film formation. Grinded samples oxidated in air and immsersed in solution generally exhibit a reduction dissolution of the oxide film, which is replaced by the growth of a new film, which usually takes a few hours [27]. OCP can be used to get an indication of the oxide stability in presence of various electrolytes [28]. In previous studies a stable OCP-value for SS 316L in static simulated milk solutions and whey-solutions is obtained after 10 hours [29], while 316L in 0.5 $\mathrm{mol\,L^{-1}}$

NaCl (approx 3 wt% NaCl) is stable after only 800 seconds [30].

2.2.2 Cyclic potentiodynamic polarization (CPDP)

Cyclic potentiodynamic polarization (CPDP) is a quick and common technique to measure pitting corrosion resistance in metals. According to the G61 standard for cyclic polarization an Avesta cell should be used. An Avesta cell has distilled water present at the O-ring fixation. This to eliminate the potential crevice corrosion between the sample/working electrode and the gasket keeping it in place. If both types of localized corrosion occurs, interpretation of the results are difficult. The procedure [31] starts with immersion of the electrodes in solution and measurement of the OCP-value. When the OCP is stable (less than $3\,\mathrm{mV\,min^{-1}}$). The solution should be purged with gas, as oxygen will make the E_{corr}-value more noble. The potential is then scanned to higher potentials from the OCP at a slow scan rate ($1.66\,\mathrm{mV\,s^{-1}}$, $\pm 5\%$), between the working and counter electrode. The scan rate has to be slow enough to that the current observed is from the corrosion reactions taking place and not the surface capacitor. Pitting and repassivation also depends greatly on time allowed at respective potential to allow for changes on the oxide layer [1]. At a certain current ($5\,\mathrm{mA/cm^2}$) or potential the scanning direction is reversed. However, $0.1\,\mathrm{mA/cm^2}$ and current densities above this being detected for 1 minute can also be used [32]. During the anodic polarization the working electrode become more anodic, or positively charged, whilst during the cathodic polarization the opposite occurs [1]. The measurement ends when either the hysteresis loop is closed or when the OCP/E_{corr} is reached, examples of curves obtained from a CPDP measurement can be seen in figure 5. The parameters obtained from CPDP are empirical and will change with varying experimental conditions.

The parameters obtained is the corrosion potential (E_{corr}), pitting potential (E_{pit}), repassivation or protection potential (E_{prot}), the potential of anodic to cathodic transition and the size of the hysteresis. E_{pit} and E_{prot} can be evaluated own or as relative to E_{corr} and are the most important parameters to evaluate pitting corrosion using CPDP. An increase of E_{pit} could indicate an inhibitory action taking place. A more noble E_{prot} indicates a lower subseptibility to pitting corrosion and a more noble E_{corr} indicates higher resistance to generalized corrosion [33]. The fact that the process of pitting is stochastically governed has been proposed to explain large deviations in E_{pit}-values from measurements [27]. The protection potential (E_{prot}) is highly correlated to the experimental conditions. It is not an intrinsic material property, instead it is dependent on the amount of propagation that occurred during the anodic sweep. Even at low potentials, sharp current increases can be observed. This can be due to defects existing on the oxide layer, resulting in a non-stable film over the passive region, where metastable pitting can initiate. In the passive region surface defects are active, resulting in propagation which can lead to an observable increased current [1]. The scan rate used during the CPDP affects the appearance of the curve [34]. Scan rates below the ASTM G61 standard are also frequently used, with $1\,\mathrm{mV\,s^{-1}}$ being commonly used [26] [35], which is the rate used in the experimental part of this report.

Hystereses has occurred when the forward (anodic) curve does not overlap with the reversal (cathodic) direction. The size of the hysteresis is evaluated based on the difference in current density at the same potentials and by integration of the hysteresis curve. A large difference indicates that the passive surface has been damaged at high potentials, also hindering repassivation of the surface. Both negative and positive hysteresis can occur, in the occurrence of localized corrosion it is always positive. A lack of hysteresis indicates that no localized corrosion has occurred, however it could be a sign of generalized corrosion and an active surface. Steps, or sudden decreases during cathodic scanning but not large enough to close the hysteresis can indicate that smaller pits repassivated, these steps are called the pit transition potentials, (E_{ptp}). Evaluating the anodic nose (anodic to cathodic transition potential) can

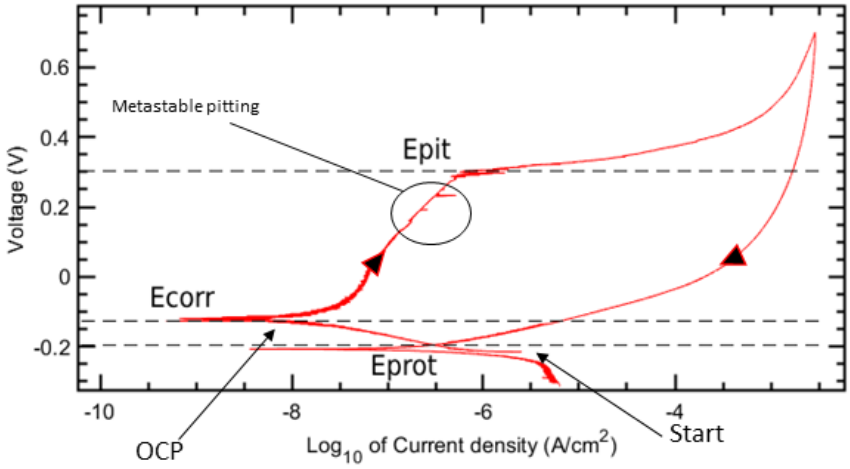

(a) Full CPDP-curve, difference between E_{prot} and E_{corr} is negative. The curve is plotted with dependent variable as x-axis which is the default way in corrosion science.

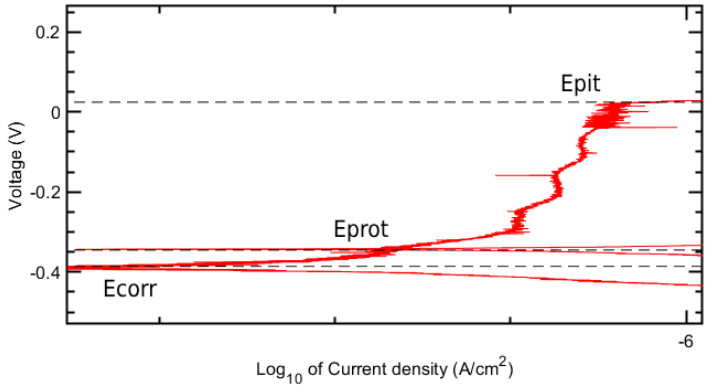

(b) Section of CPDP curve, difference between E_{prot} and E_{corr} is here positive. The current transients indicate metastable pitting below E_{pit}, visible in both a) and b). It is encircled in a) and is the current transients.

Figure 5: Exampled of CPDP curves, with denoted important potentials for evaluaiton of localized corrosion.

indicate which metals and electrolyte combinations that allow for restoration of the oxide film [33].

Polarization resistance (R_p) can be used as a complement to pitting potential to evaluate inhibition. It is defined as the resistance of a specimen to oxidation during polarization and can be obtained from the CPDP-curve. In small vicinity ($\pm$10mV) of the E_{corr}/OCP the response is linear, and the inverse of the slope is the R_p, which depends on both the sample and electrolyte. This method can be used to evaluate inhibitor efficiency [36], however the same electrolyte has to be used to evaluate only inhibitor efficiency. The inhibition occurring at potentials close to the OCP/E_{corr} does not guarantee that the same inhibition occurs across all potentials. Eq 8 can be used to calculate the percentage inhibitor efficiency (%IE) R_p, in which the polarization resistance is compared with and without inhibitor applied [37].

$$\text{IE}\% = \left(\frac{R_p(\text{Inhibitor}) - R_p(\text{Without})}{R_p(\text{Inhibitor}) \times 100} \right) \tag{8}$$

2.3 Corrosion testing machine (Sören)

To realize non-static corrosion measurements during simulated processing conditions a test method and setup consisting of an Armfield FT74 pasteurizer (also denoted *Sören*) with a test chamber coupled to an external potentiostat for electrochemical measurements and cooler was developed in 2022 by a master student, Tetra Pak and the division of Production and Materials Engineering at Lund University [10]. Utilizing a pasteurizer allows for rapid heating and cooling of the test solution. Milk and similar dairy products cannot withstand heat for an extensive time without alterations to the product which is the reason for rapid heat treatments in industry, described in short in section 2.5. The rapid cooling of product allows the method to simulate continuous processing conditions whilst not requiring enormous amounts of solution to pass through the test chamber. The test chamber allows for easy changing of samples however the flow geometry and deviation from the recommended [31] Avesta cell can result in crevice corrosion. Temperature and pump frequency can be controlled by the pasterurizer and the coupled computer and potentiostat allows for application of potential to monitor the resulting current, ie. corrosion occurring at the sample surface. More details on the components used and settings is presented in section 3. Images of the entire setup is presented in figures 6, 7 and 8.

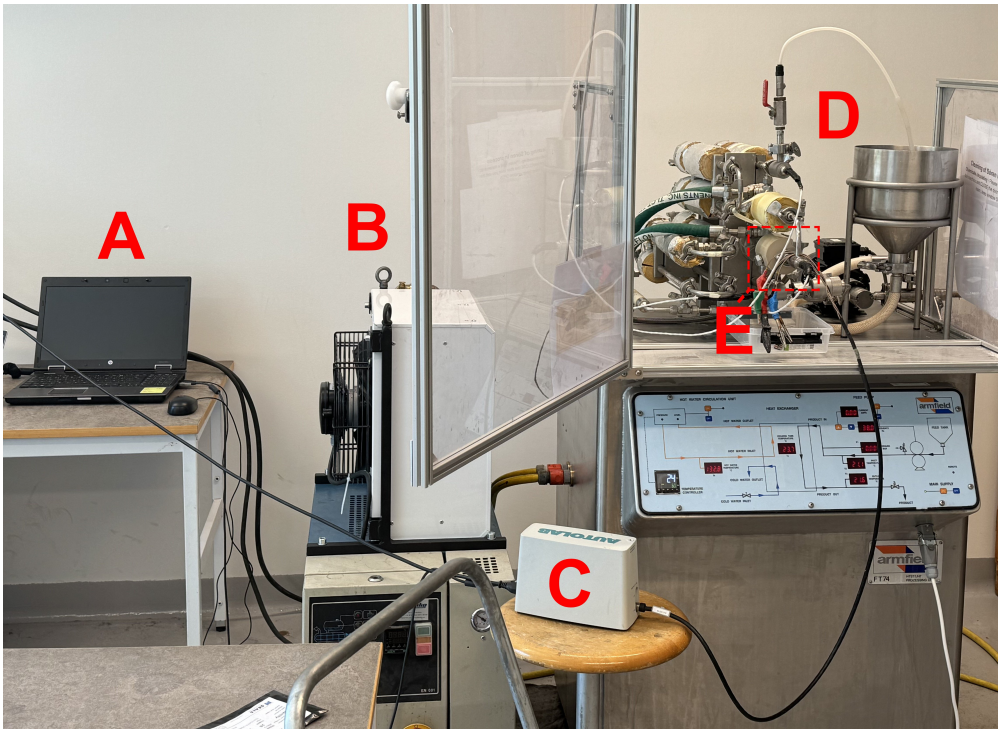

Figure 6: Corrosion testing machine and setup. A: Computer controlling the potentiostat. B: External cooler. C: Potentiostat. D: Corrosion testing machine, pasterizer Armfield FT74 E: Test chamber, electrode connection. Machine is not operating in the image.

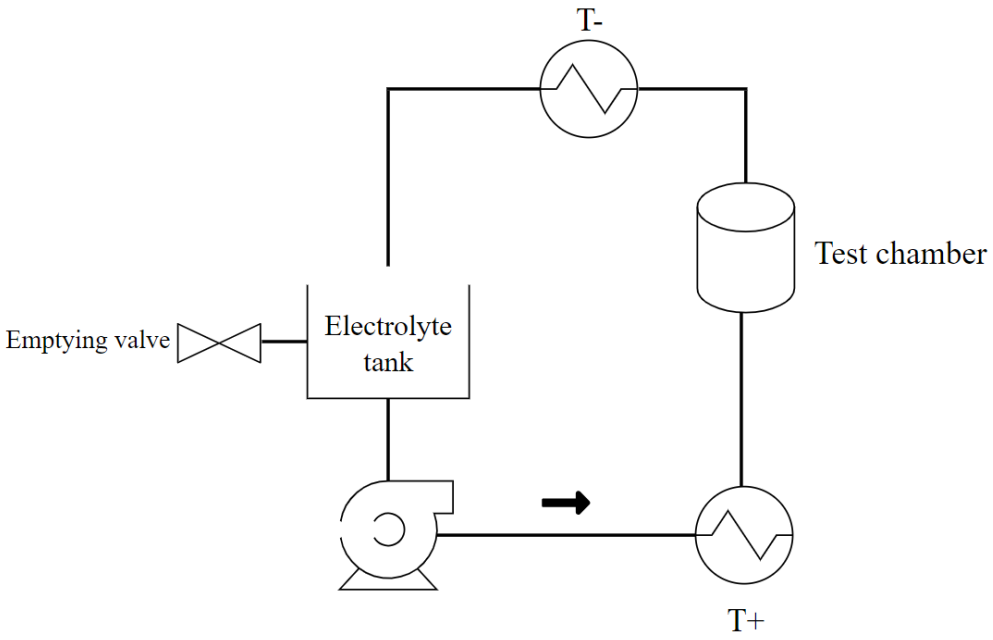

Figure 7: Schematic flow chart of experimental setup in the Armfield FT74 pasteurizer. The solution is feeded from the tank to the pump where the solution is then pumped, heated in a tubular heat exchanger. The solution passes the test chamber and is subsequently cooled in a tubular heat exchanger and returns to the electrolyte tank. The system is emptied by the valve close to the tank.

Figure 8: Close ups of setup. To the left, close up of attached test chamber, isolated piping and electrolyte tank. To the right, attachment of electrodes to potentiostat, not attached to corrosion testing machine. Counter electrode (black), reference electrode (blue) and working electrode (red).

2.4 Stainless steels

Stainless steels are utilized for many different applications due to their high mechanical strength, machinability and excellent corrosion resistance. Stainless steels are however susceptible to localized corrosion, at specific sites where the passive film fails [38], as mentioned in section 2.1.1. Stainless steels are by convention categorized as stainless if the alloy contains minimum 12wt% chromium and maximum 1.2wt% of carbon [2]. Attributes of the material, material chemistry and mechanisms of inhibition of corrosion on stainless steels is presented in the following section.

2.4.1 1.4404 ASTM 316L Stainless Steel

SS 316L/316 is a chromium-nickel-molybdenum doped austenitic stainless steel with the composition presented in table 1. The austenitic structure is due to the additon of nickel that stabilizes the FCC/austenitic phase. This also makes the alloy non-magnetic and non-supsebtilbe to heat treatment hardening. It is well suited for process streams containing chlorides and halides, due to the addition of molybdenum resulting in its resistance to pitting and general corrosion. The alloy is often dual certified as 316 and 316L, with the addition of nitrogen to the 316L (*L* for low carbon), 316L can meet the mechanical properties of 316. It is easily processed and welded by standard practices. In general, SS 316L performs superior compared to SS 304, however in presence of nitric acid stainless steels containing molybdenum perform worse [39].

Table 1: Chemical composition of Stainless steel 1.4404 ASTM, supplied by manufacturer Tibnor (2024) [4] and reference values [5].

Chemical composition (wt%)										
Element	Fe	C	N	Cr	Ni	Mo	Mn	S	P	Si
Manufacturer	69.42	0.02	0.06	17.3	11	2.2	-	-	-	-
Literature	Bal	0.03	0.10	16-18	10-14	2-3	2	0.03	0.064	0.75

The alloying elements are to varying degrees beneficial and not beneficial in terms of passivity. The addition of chromium eliminates the general corrosion. Chromium is almost always beneficial in terms of passivisation but molybdenum is only beneficial when chromium is present, an effect noted for binary and ternary alloys. Molybdenum is suggested to cover active sites, inhibiting attack, both as a salt in solution and as an ion dissolved in the alloy. Molybdenum is also proposed to interact with cation vacancies in the passive film, reducing the flux of cation vacancies to the metal. The ions might also limit chloride migration through the passive film [1]. Molybdenum has also been proposed to aid in repairing the passive film [40]. Silicon is also be added to increase corrosion resistance for stainless steels to be used in sulfuric acids [41]. It has also been showed by electron diffraction that as chromium is progressively added to iron, that the passive film becomes more amorphous, as compared to poly crystalline. With other findings it has thus been proposed that the structure of the passive film has an impact on how well the passive film performs. An amorphous film does not have grain boundaries and defects such as poly crystalline materials, which can facilitate ion migration across the film [1].

The composition of passive films in stainless steels does not only depend on alloying elements. The oxide film and stability is highly dependent on the environment in which it is formed, reformed and utilized as it is in a constant breakdown and formation cycle. Passive films are usually a few nanometres thick and is composed of metal oxides, hydroxides and oxyhydroxides. Water may also be bound in the passive film [1]. A general theory which has been confirmed by XPS and ToF-SIMS for SS 316L is that the passive layer consists of a bilayer structure. The outer layer consists of hydroxides and oxides with Fe(III) and Mo(IV,VI) species and the inner layer with Cr(III)-oxide species. This passive film forms readily in air and ambient temperatures. To further strengthen the passivity of the oxide film passivisation in acid is a common procedure [40], this increases the stability of the oxides. It has been reported that passive films on stainless steel when immersed in water will reform, and that the formed passive layer is more susceptible to localized corrosion [27]. Iron oxides are dissolved, freeing electrons that then can react with the chromium(III)oxide to free chromium ions, that can migrate and enrich the outer iron oxide [27]. However, this mechanism is to mostly present for SS 3014 as the molybdenum in 316L stabilizes the iron and limits the dissolution [42]. The passive behaviour of SS is often contributed

to the Cr_2O_3 species in the inner layer of the passive film however the mechanism is still unknown. It has been proposed that the recovery of metastable pits is more important than the ability of the film to withstand aggressive species [43]. The stability of present chemical species in the system depends on the potential and pH of the system which is described in experimentally produced Pourbaix diagrams that can be used when designing electrochemical measurements per example.

To confirm the chemical composition as supplied by manufacturer and for literature values, X-ray flourosence spectrometry (XRF) and Laser Induced Breakdown Spectroscopy (LIBS) can be used. XRF is a common technique for elemental composition in both industry and academica. Depending on instrument, XRF can detect elements down to 1-10mg/kg. Using a source of X-ray photons the inner shell (k,l,m) electrons of an atom are ionized, this is unstable and decay is immidate. A transition of an outer shell electron falls down to fill the vacancy, emitting a X-ray photon. The energy of this emitted photon is characteristic to the element and quantity of it [44]. LIBS can compared to XRF detect elements with lower atomic weight than sodium, such as carbon [45]. It operates by applying a high-focused short lived laser on the surface of the sample, resulting in a small loss of mass on the surface. This mass interacts with the laser forming a plasma, containing atoms, ions and electrons. This cools down, resulting in that the excited species fall down to stable energetic levels, emitting light with characteristic wavelengths, which can be used to detect and quantify elements [46].

2.4.2 Inhibiting localized corrosion on stainless steels

Inhibitory effects on pitting corrosion can be obtained in many ways. The following section explores inhibition that can occur without alteration of electrolyte salt concentration. The main cause of pitting corrosion on stainless steels are manganese sulphide (MnS) inclusions. These impurities disrupt the passive film layer where pitting then can initiate. The inclusions are unstable in the chloride rich environments in the propagating pits [1]. When the MnS inclusion dissolved the metal matrix becomes exposed allowing for attack by chloride ions and sulfur containing species (from the MnS dissolution). This results in a micro crevice and when the the crevice reaches 1 µm the stable pit may propagate [2]. Localized corrosion can be inhibited by the presence of an inhibitor. Effective corrosion inhibitors are in general organic compounds with structures containing delocalized electrons or free electron pairs such as pi-bonds, aromatic rings and heteratoms such as nitrogen, oxygen and phosphoros. These can adsorb on the metal surface and by blocking active areas on the steel surface inhibit corrosion reactions [47]. Inorganic species such as chromate, nitrite and molybdates have also proven to inhibit pitting corrosion. In food processing applications with strict contamination and toxicological guidelines, most inhibitors and/or coatings are unsuitable [48]. However food products can contain species able to inhibit pitting corrosion. A few examples of molecules present in milk with aromaticity, π-bonds and/or C-OH bonds are depicted below in figure 9. Dairy products are complex and according to the milk database established by A Foroutan. et al [49] 51 species present in commercial cows milk contain aromatic rings, 109 species contain a C-OH bond and 73 structures contain a double bond [49], all of which could be potential inhibitors. More on composition, microstructure and processing of dairy in section 2.5.

In the case of SS 316L, a few organic molecules has been reported to be effective inhibitors. In a study by Alahiane et al. benzoic acid was determined to be an excellent inhibitor off 316L in H_2SO_4 solution. The experimental tests (electrochemical methods and SEM) was compared to molecular dynamic, monte carlo and density functional theory computations and the results overlapped. They showed that the surface contact between the benzoic acid derivates were optimal allowing for formation of bonds by the donor atoms (oxygen) to the vacant orbitals of iron [50]. In another study by Sanni et al. egg shell powder in NaCl solutions were found to effectively inhibit corrosion on 316L. The SS surface

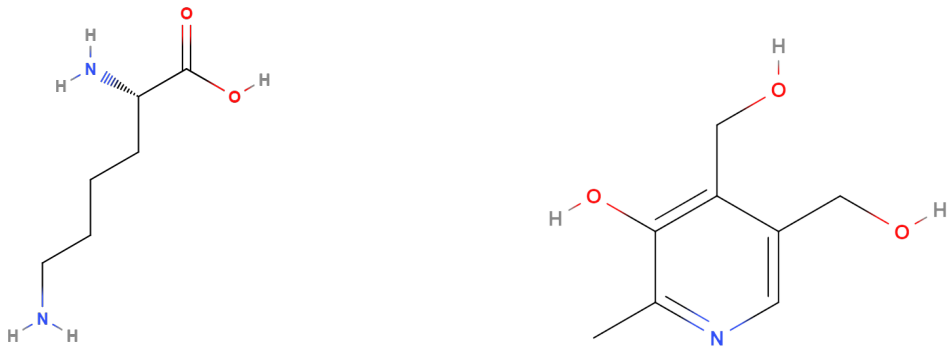

Figure 9: Example of molecules in commercial cows milk containing electron dense areas. The amino-acid lysine (left) is an effective inhibitor on SS316L in 0.5M NaCl-solution [3] and Pyridoxine (right) with characteristics that could inhibit localized corrosion.

in presence of optimal concentration (as detemined by electrochemical measurments) was smooth in comparison to the control sample and the concentration of chlorides on the surface had decreased as per SEM and EDX respectively. The mechanism was assumed to be adsorption but no comments were made on the chemistry at the surface [51]. Other organic compounds to have inhibited corrosion on SS 316L are aminoacids (L-lysine and L-arginine) for pitting corrosion in 0.5 mol/L NaCl-solution [3], 2-mercaptobenzimidazole for pitting corrosion [52] and even various food additives (also safe for consumption) for general corrosion [53].

2.5 Dairy chemistry and interaction with stainless steels

The following section describes dairy chemistry and how it can interact with stainless steel surfaces.

2.5.1 Dairy chemistry

Dairy products are chemically complex colloidal system consisting of minerals, proteins and carbohydrates being either dispersed or dissolved in a continuous aqueous phase. The major chemical constituents of whole milk are carbohydrates (lactose, galactose and glucose), minerals and ions (calcium and potassium), and amine-containing organic metabolites (creatine, choline, urea). Other components are mono, di & tri-glycerides (fats), amino acids and vitamins. More than 2355 different chemical components has been detected in Bovine milk and 1705 of these has also been quantified [49].

The ionic conductivity of a solution is increased with increasing of milk concentration and temperature. An effect assumed to derive from that the concentration of ions and mobility within the solution increases with the two factors. However viscosity likely reduce ionic conductivity to a certain degree [54]. The pH of milk is usually around 6.5-6.7 due to lactic acid (a few milligrams per 10(0 g of whole milk [49]), with increasing temperature and pressure the pH decreases linearly. In the range 40 to 80 °C the linear coefficient has been found to be -0.0078 pH unit/°C [55].

Common milk processing procedures are various types of thermal treatment. The European recommended pasteruization standard is the high-temperature short-time during which the milk is heated to 72-74°C for 15-20s. An alternative is heating to 62-65°C for 30min. Cream pasteurization is done at

75-80 °C for 30s and ultra high temperature pasteurization (leading to sterile product suitable for stage in room temperature) is performed at 135-1(50 °C for only a few seconds. Whey proteins are denatured and partakes in agglomeration at temperatures above 65°C, with variations depending on protein type. Heating also induces minerals to precipitate and these can be deposited on walls of heat-exchangers as fouling [56], which is presented further in section 2.5.4.

2.5.2 Skim Milk Powder (SMP)

Skim milk powder is the product derived when removing the majority of fat and water from milk. The major component of dried milk products is amorphous lactose with protein, fat and air being dispersed in the lactose. The general chemical composition of skim milk powders can be found in table 2. The physical properties of the powder is strongly dependent on the structure of the lactose.

Table 2: Composition of skim milk [6].

Chemical component	**Concentration (g/10**(0 g)
Moisture	3.2
Protein	36.2
Fat	0.8
Carbohydrates/lactose	52
Minerals (ash)	7.9

Addition of salt (NaCl) to SMP alters the equilibrium and structure of casein micelles. There is no difference in size of micelles however the effective charge is altered and the pH is somewhat decreased when added to SMP-solutions [57].

2.5.3 The milk and metal interface

Milk products contain surface active agents (for example fats and proteins) and how well these adhere depend on among other factors composition of the product [58]. The reactions occurring at the interface between dairy and stainless steels are essential to consider in choosing materials for processing equipment. These vary between different steel grades and this was studied by Atapour et al. in 2019. They followed metal release, changes in corrosion behaviour and surface composition of different steel grades in simulated milk solutions (SMS) and whey solutions. They found that the rate of general corrosion was low in all grades (LDX 2101, AISI 316L and AISI 430) and that pitting only occurred in SMS for AISI 430, for the set conditions. All grades exhibited an increase of chromium in the passive oxide layer by XPS analysis. The AISI 430 exhibited worse passive layer performance compared to the other grades, which is reportedly due to the presence or molybdenum in grade 316L and more chromium in grade LDX 2101. A higher metal release was noted in the whey solution compared to the SMS for all steel grades. Metal release in relation to protein content is hypothesized to be governed by different mechanisms and processes, which in some cases are contradicting [59]. In another study it was also found that 316L released higher amounts of metal in contact with whey solutions, ie. solutions containing more protein. The effect was mostly evident after 24 hours during stirring and 48 hours during static conditions. It was also found that the oxide layer became thinner and more enriched in chromium. Stirring conditions resulted in an increase of metal release and once released the metals aided in precipitation and formation of protein agglomerates. These clustered molecules then caused wear to the metal surface. An increase

of protein in solution resulted in a lower OCP-value, which aligned with the metal release observed in the study [29]. Stainless steel surfaces can be ”conditioned” in contact with a liquid medium in which adsorbed molecular species such as proteins alter the physicochemical properties of the surface [60]. It has also been reported that purposefully conditioning stainless steel surfaces with milk and milk proteins limits adsorption of bacteria, however the effect only lasts 30 minutes [61]. Although not directly correlated to pitting corrosion, the research on biofilms and primarily conditioning can confirm that proteins attach to stainless steel surfaces [60] [61], which also is observed in industry [62].

2.5.4 Fouling

Fouling by milk products is a common phenomena in stainless steel heat exchangers during pasteurization. Factors determining the degree of fouling is pH and temperature, which correlate to the degree of protein denaturation in the solution. Calcium phosphate is also a common component in the fouling deposit, which also agglomerate due to heating. In the initial stages of fouling single non-agglomerated proteins adhere to the heated stainless steel surface, once the surface is covered the agglomerated proteins and calcium phosphates adhere to the surface. Adhesion starts at room temperature for whey proteins, however bulk fouling is not instant, the adhesion of proteins only alters the surface by presumed chemical linkage. The protein-modified surface is thought to be the basis of further colloidal attachment. It has also been found that heating the milk to 80-85°C for 5-10 minutes before entering the heat exchanger reduces the fouling to a predominantly mineral one, as the proteins have been predenatured. The lag time, or time it takes for significant deposit of fouling, depends on how rapid the formation of agglomerates is, with factors such as pH, heating and mixing of the solution affecting it. The chemistry of the product affects the particle formation, and fouling can thus vary with seasonal changes in the milk processed. It has also been noted that tubular heat exchangers experience a longer lag time due to inefficient mixing compared to plate heat exchangers. [63].

2.5.5 Biofilms

Adhesion of bacteria to stainless steel equipment surfaces is common and can be a concern if not cleaned correctly. The first step of biofilm formation is conditioning and depending on surface roughness and adsorbed species (among factors) the rate of film growth can vary [60]. Biofilms can once established induce pitting corrosion. It has been reported for stainless steels of grade 304 and 316 during processing of dairy products. In a coupon study, single types of bacterium and sporophorms resulted in similar pitting corrosion of both polished and non-polished steel coupons. The coupons were left in contact to different bacteria for up to 8 weeks, in general the highest viable count of bacteria in respective biofilm was the highest at 6 weeks [64]. Biofilms will likely not form on the samples, however the setup might experience biofilm growth [65] which could affect the experiments.

3 Method and experimental design

The following section encompasses how the experimental part of this report was planned, conducted and how the resulting data was analyzed. For a more in-depth operating procedure refer to the separate operating guide.

3.1 Design of experiment

The design of experiment (DOE) was based on a full-factorial design with levels of interest. The DOE is based on processing conditions however the maximum temperature assessed is well below 140°C (UHT [56]) and the maximum salt concentration assessed is well above expected salt range during processing of dairy products. Extension and limitation of processing factors were based on previous corrosion testing of salt solutions [32] [10] and ease of operation of the corrosion machine, for example a higher temperature would likely induce more fouling [56], require an increase of the cooling efficiency and require harsher cleaning routines of the setup.

The factors studied were milk concentration, salt concentration and temperature. By varying the milk concentration the potential inhibitory effect could be compared for different salt concentrations and at different temperatures. The salt and temperature levels were partly based on previous parameters and findings using the corrosion testing machine by a previous master student [10], and is aligned with common processing temperatures for dairy products. The temperatures assessed were 30 °C, 60 °C and 80 °C. The assessed salt concentrations were 10 ppm, 100 ppm, 1000 ppm, 10 000 ppm and 100 000 ppm. The highest milk-concentration was based on recommended dosage by manufacturer, which correlates to 96 g of dry product/950 mL of water. The other milk concentrations were 55 g/950 mL (57 %),24 g/950 mL (25 %) and 0 g/950 mL (0%). Since the skimmed milk-powder contained 1.1 g salt per 100 g dry product, the lowest salt concentrations were only possible for measurements where low or no milk was present in the electrolyte. The varied milk-concentration accounted for the total variation of fats, proteins and carbohydrates, as these were not added independently. The full-factorial design was created using the function *fullfact* in MATLAB R2022a. The resulting sample space can be seen in Figure 10 and each point represents three samples, in total 129 samples.

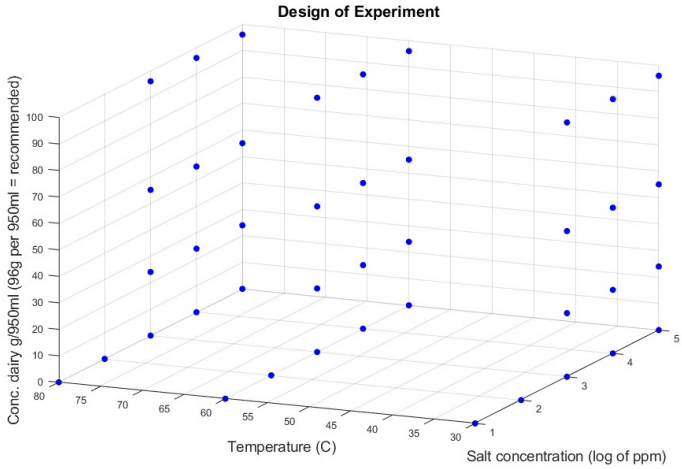

Figure 10: Sample space for the experiment, each point corresponding to three measurements. Based on a full-factorial design, the space is uneven due to native salt content in the dairy product used.

3.2 Experiment

3.2.1 Sample preparation

The stainless steel samples of type ASTM 316L were prepared continuously, to allow for minimum 7 days and maximum of 10 days of surface oxidation before each measurement. The samples was cut into 13mm long rod pieces and was placed in the sample holder and grinded using a Struers Tegramin-30. Silicone carbide paper with 220 grit was used and the samples were grinded at 200 rpms (revolutions per minute) with water until the sample surface was evenly grinded, see figure 11 for utilized sample holder and grinded sample. The average surface roughness (Ra) was measured using an optical microscope and determined to be (0.7 µm), which is below the critical limit (0.8 µm) for steels used in food applications [66]. The samples were subsequently ultrasonically cleaned in ethanol (80 wt%) for 5 minutes. The samples were air-dried and left to oxidize for at least 7 days in a sealed plastic bag wrapped in a clean room cloth. Before measurement the samples were rinsed with distilled water. The exposed surface area of the sample in the test chamber was 0.385 cm^2 however it varied some due to heat induced pertubations of the O-ring. This resulted in a smaller exposed sample surface, resulting in that the cutoff during polarization would be slightly too high. The chemical composition was confirmed using Sciaps handheld XRF and LIBS-analyzers of the types X505 and Z-903 Carbon+ respectively.

Figure 11: Grinded sample and sample holder used to grind samples.

3.2.2 Electrolyte

Water, salt and skim milk powder were weighed and mixed with a magnetic stirrer for at least 15 minutes before measurements. The salt used was *Falksalt hushållssalt* without iodine. The salt contained 99.8g salt and 0.2 g of anti-caking agent sodium feorrocyanide per 10(0 g product. The skimmed milk powder was from the manufacturer *Semper Mjölk*, with the chemical composition presented in Table 3. Both products are commercially available as of May 2024. The moisture content of the milk powder (3-4 wt%, [67]) was not considered in concentration calculations.

Table 3: Composition of Semper skimmed milk powder [Semper, 2024]. The product also contains Vitamin B12 and calcium per example.

Component	**g/100g dry product**
Fats	1.0
- Saturated fats	0.7
Carbohydrates	51
- Sugars	50
Protein	36
Salt	1.1

3.2.3 Setup of dynamic corrosion measurements

The corrosion testing machine (adjusted Armfield FT74 pasteurizer coupled to an external cooler) was used for the measurements. For the electrochemical measurements an Autolab PGSTAT101 and the software NOVA 2.1.7 was utilized. A three electrode setup, with an Ag/AgCl reference electrode and a glassy carbon counter electrode was used, see figure 12 for a simplified schematic and image of the test chamber. The working electrode was the prepared steel sample fastened by a steel screw. The approximate distance between the reference electrode and the working electrode was 4mm. The pump frequency was set to 30.8 Hz which corresponded to a flow rate of $1.2\,\mathrm{L\,min^{-1}}$, see figure 7 for a simplified flow chart. When the system reached the set temperature, a 30-minute OCP-measurement was conducted followed by CPDP. The starting potential was -0.2 V vs OCP above -0.55 V (hydrogen evolution potential), to allow for a safety margin if the measured OCP value was to high. The scanning direction was reversed when the current density reached $5\,\mathrm{mA/cm^2}$, which for this system was set to 1.925 mA, in accordance to the ASTM standard for cyclical polarization [68]. If the cutoff was not reached, the scanning direction was reversed at 0.7 V which is 0.1 V below the oxygen evolution potential. The measurement was either ended manually or automatically when the potential reached -0.2 V vs OCP or when the hysteresis loop was closed. The machine was emptied and at least 4 L water were pumped through the machine, the test chamber was removed and rinsed and the O-ring and electrodes were cleaned with a damp clean-room cloth after each measurement.

3.2.4 Cleaning in place

A cleaning in place (CIP) routine was followed to clean the pasteurizer. The routine was performed on average every 30 measurements, or when needed. To keep the premise of process-like operating conditions, the routine largely followed industry practice with adjustments made to suit the pasteurizer and operating conditions. The test chamber was assembled as normal but without the electrodes, which were replaced by screws. The routine consisted of four subsequent steps with the first being a rinse of approximately 4 L water at room temperature. After this NaOH (1 wt%) was circulated in the system at 50 °C for 60 minutes. The system was then rinsed with water again followed by HNO_3 (1 wt%) circulating in the system for 40 minutes, at 50 °C. The system was after this rinsed with water again and the acid was disposed in suitable storage.

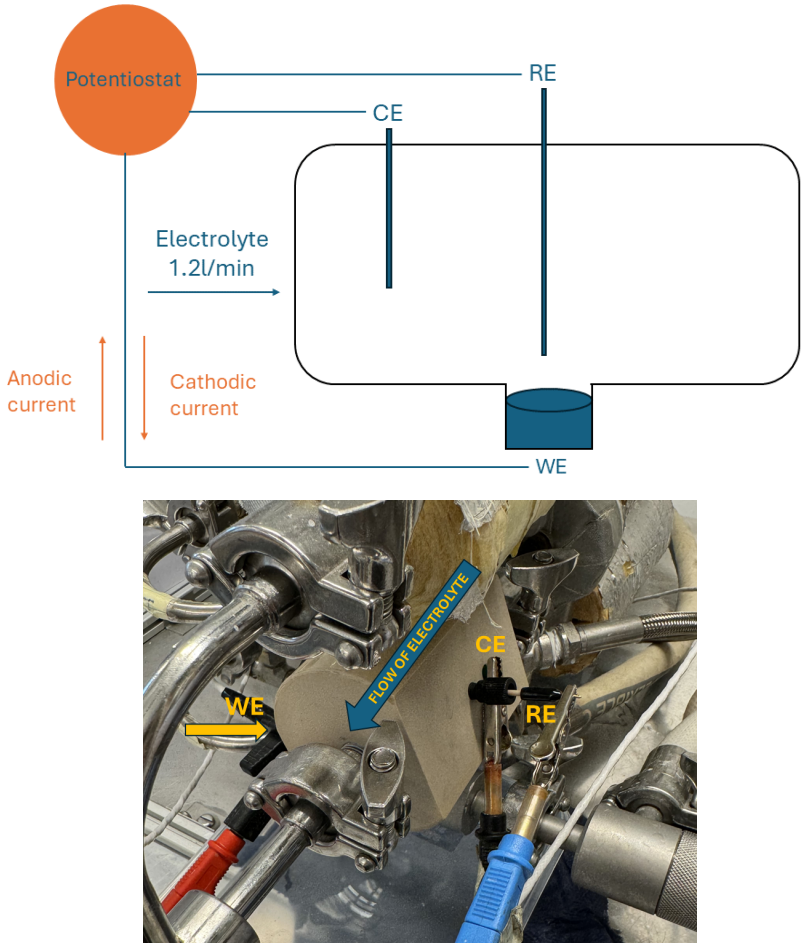

Figure 12: Simplified schematic of the three electrode setup inside the test chamber, wiring from electrodes and an image of test chamber during measurement. Anodic scanning is current flowing from WE to the CE through the external circuit, while cathodic scanning is current flowing from the CE to the WE through the external circuit. The circuit is closed via the ions in solution.

3.3 Data evaluation

The resulting data from the software NOVA 2.1 were evaluated in MATLAB R2022A with the *Statistics and Machine learning-toolbox*. The distribution of the data (see Appendix A1) was assessed using *Adtest* (Anderson-Darling test) and *Normplot*. To analyze the significance across varying parameters an ANOVA and following post-hoc test was utilized. The functions used were *Anovan* and *multcompare*. For general standard deviations the function *std* was used and paired t-tests were performed using the *ttest*-function.

4 Results and Discussion

4.1 Chemical composition of SS 316L

The chemical composition from the XRF and LIBS-measurements and the previously reported composition from manufacturer and literature value [5] can be seen in table 4.

Table 4: Chemical composition of SS 316L (wt%), from manufacturer Tibnor (2024) and measured with XRF and LIBS.

Chemical composition of SS 316 (wt%)				
Element	**Manufacturer**	**Literature [5]**	**XRF**	**LIBS**
Fe	69.42	69	68.46	-
Cr	17.3	16-18	16.81	-
Ni	11	10-14	10.01	-
Mo	2.2	2-3	2.05	-
Mn	-	2	1.39	1.40
Si	-	0.75	0.511	0.493
N	0.06	0.10	-	-
P	-	0.045	0.064	-
C	0.02	0.03	-	0.023
Cu	-	-	-	0.325
V	-	-	0.059	-
S	-	0.03	0.137	-

Both of the measurements roughly coincide with the reported contents by the manufacturer. By LIBS the low-carbon content could be confirmed, which is an important property of 316L SS. The XRF reports a sufficient chromium concentration to obtain the characteristics of SS 316L [5] with the passive oxide layer mentioned in section 2.4. The silicon is likely lower than expected in the utilized SS316L than indicated by literature which can affect the corrosion resistance [41]. The nitrogen content could not be confirmed with either XRF or LIBS. The measurements coincide with literature and manufacturer specification and can likely be compared with other SS 316L components used in food industry.

4.2 Effect of chloride concentration and temperature on pitting corrosion of SS 316L

Based on all 129 measurements there were significant differences induced by temperature and salt across all levels indicated by an N-way ANOVA at a confidence level of $\alpha = 0.05$. See p-values in appendix A1. Throughout the results the confidence level of 5% was used since it varied withing subgroups. The inhibitory effect on pitting corrosion of SS 316L was evaluated by comparing the corrosion parameters with and without milk powder present in the electrolyte.

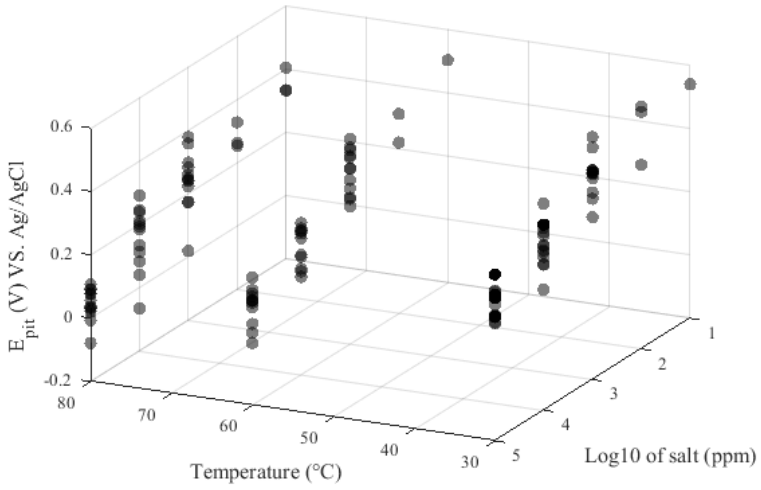

Figure 13: All measurements. Within each parameter set at salt concentrations 1000 ppm, 10 000 ppm and 100 000 ppm all milk concentrations were assessed and the variation in E_{pit}-values hint at the inhibitory effect presented in section 4.2.2.

The OCP and E_{corr}-values did not always coincide. The differences could be explained by method sensitivity at low currents, the scan rate [26] and the dynamic environment during measurements. The oxide layer and/or other surface conditions could change during the time frame of immersion and measurement of OCP and CPDP which would lead to differences in measured values. The sensitivity of the method could also result in differences as the currents observed when measuring OCP and E_{corr} are very small (often in the range of $10^{-10}A$) and the signal could be interfered with by local and instant changes in for example the electrolyte. Across all measurements OCP and E_{corr} exhibited some differences. Using a paired t-test the two exhibited significant differences. See figure 14 for the difference between OCP and E_{corr}-values measured.

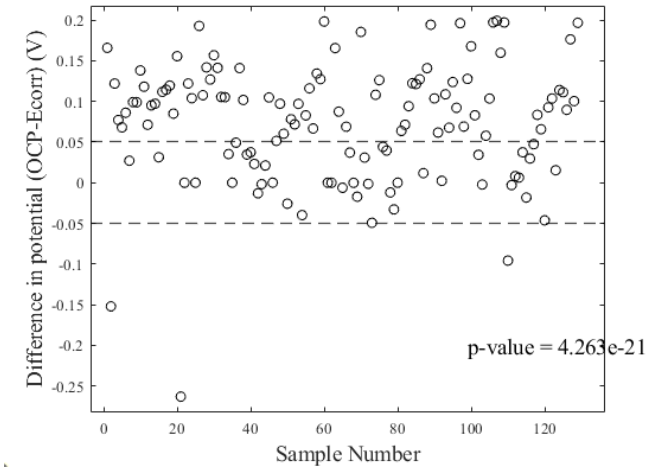

Figure 14: All samples and the difference between OCP and E_{corr}, OCP- E_{corr}. The two dashed lines indicate samples where the difference is ± 0.05. A majority of the differences are bigger than this.

There was a significant difference for OCP-E_{corr} for 80 °C and 60 °C however not for 30 °C versus the other temperatures and the cause for this is unclear. 100 000 ppm was significantly different from

the other salt concentrations. The smallest differences between OCP and E_{corr} were for the highest temperature and highest salt concentrations. See appendix A1 for a post-hoc test for OCP-E_{corr}.

Evaluating the OCP and E_{corr}-values indicated differences between temperatures and salt concentrations. On OCP the significant differences were found between 30 °C and 80 °C and for E_{corr} it was found between 30 °C and 60 °C. For the OCP-values the solutions with 100 000 ppm salt concentrations resulted in significantly lower E_{corr}-values compared to the other concentrations. See appendix A1 for post-hoc tests of OCP and E_{corr}. The effects in solution, effects on the SS 316L oxide layer and interactions at the interface are complex and would require complementary analytical techniques to be further investigated. For example ionic species present could attribute to differences in the EDL, affecting the ion migration to and from the SS-surface [1]. The oxide layer might also be affected and altered by temperature and by oxygen dissolved [69] in the solution, which is altered by both temperature and salt concentration [70]. Since general corrosion, which is quantified using the corrosion potential/OCP-value is usually not a problem in processing equipment it might only be necessary to make sure that the values obtained are stable. This to simulate the food processing system at hand where immersion of the steel in solution is often longer than during measurements using the corrosion testing machine. The immersion time will likely matter since it has been reported that the oxide layer on SS 316L in milk solutions and during stirring [29] takes a longer time to stabilize. It is ideal in terms of simulating real processing conditions to conduct the electrochemical measurements on a oxide layer similar to the one obtained in industry, where the immersion time likely is longer than the 30 minutes of OCP-stabilization used in this report. Since this immersion time is shorter than the estimated time for oxide stability in milk solution (10h static solution, [29]) this could affect how ”industry relevant” the results are.

4.2.1 In water solutions

Based on 45 measurements in water with varying concentrations of salt and temperatures there were significant ($\alpha = 0.05$) differences between the pitting potentials for the SS 316L samples based on salt and temperature. This has already been established [10], however not with the updated sample preparation routine of grinding to food equipment standard surface roughness. The temperature levels were all significant however 10 000 ppm and 100 000 ppm did not exhibit significance. However they do when comparing all measurements, indicating that the sample size is important using this experimental method. There was also a significant effect on E_{pit}-E_{corr} at the same significance level for temperature and salt concentration. See figure 15 for E_{pit}-values measured. A few measurements did not exhibit pitting for all replicates and these replicates are excluded.

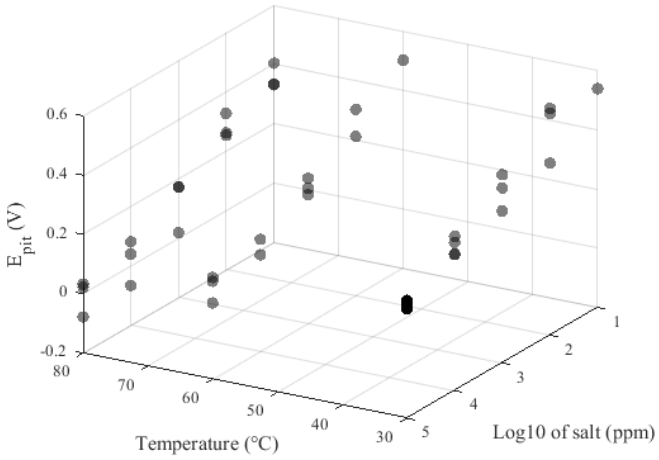

Figure 15: All measurements without milk. At 10 ppm and 100 ppm no E_{pit} was detected for certain combinations. For example at 60 °C and 10 ppm only one measurement exhibited pitting below the oxygen evolution potential.

On E_{corr} alone in water solutions there was no significant differences induced by temperature and salt concentration. The E_{pit}-E_{corr} is likely significant due to the E_{pit} contribution in water solutions. This could be due to sensitivity of method and sample size, since some differences were present when looking at the whole dataset. In static solutions OCP/E_{corr} should be stable for 316L during the time frame of the experiment in salt-water solutions [30], however non static conditions could also the values obtained. The repassivation potential E_{prot} were not evaluated with data analysis and most of the values were below respective E_{corr}-value. This was likely a result of a to high cutoff during the anodic scanning. For future CPDP-measurements it would be beneficial to lower the cutoff based on current to more accurately evaluate repassivation and hysteresis. The pitting potential (E_{pit}) decreased as expected when samples are exposed to higher temperatures and salt concentrations [10] [2]. See figure 18 for an example of how the CPDP curves varied with different salt concentration.

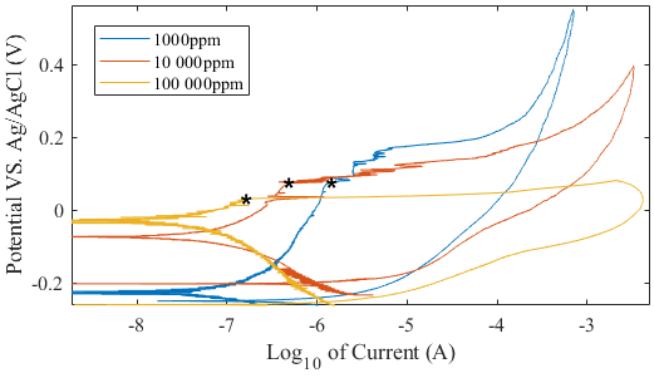

Figure 16: CPDP curves for varying salt concentrations in water at 80 °C. Examples of where E_{pit}-values where extracted is marked with stars. Notably in regions with unclear exact pitting onset the middle lowest value were chosen, see for example 1000 ppm curve.

E_{pit} is in expected order, with the highest salt concentration contributing to the lowest pitting potential. E_{corr} is in opposite order, with the highest salt concentration being the highest. This indicates (for these measurements) that the general corrosion occurs at lower potentials for 1000 ppm compared to the

higher concentrations. This effect is not expected and could be due to oxide stability varying between the samples due to sample preparation per example. See figure 17 for examples of CPDP-curves at 30 °C with varying salt concentrations.

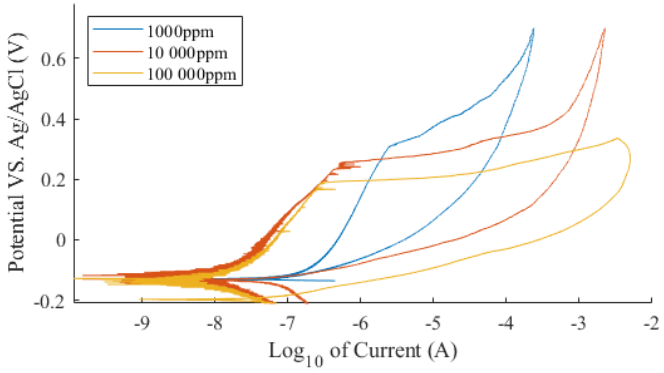

Figure 17: CPDP curves for varying salt concentrations in water at 30 °C.

The size of hysteresis, measured as the difference in current density between the same potentials in the loop, increases in the two examples of measurements with salt concentration for both 30 °C and 80 °C. The size of the hysteresis is the largest for 100 000 ppm. A lot of the measurements indicated metastable pitting. Both of these are expected effects [2], however they were not statistically evaluated.

As mentioned temperature also affects the pitting potential and corrosion behaviours of the SS 316L significantly, an example of CPDP-curves for varying temperatures at the same salt concentration (1000 ppm) can be seen in figure 18.

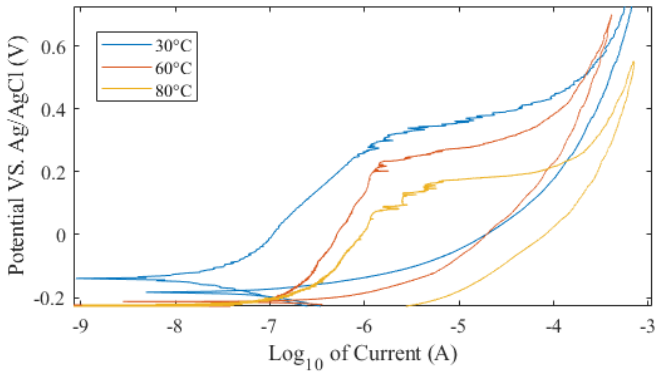

Figure 18: Varying temperatures for water solutions containing 1000 ppm salt.

Increasing the temperature does not seem to induce the same degree of hysteresis as increasing the salt concentration does. Both contribute to an less noble onset of pitting, however the salt contributes to an increased risk of susceptibility to pitting which is indicated by large hysteresis [33]. The E_{corr}-value of 30 °C is more noble compared to the values of 60 °C and 80 °C. This is expected since general corrosion is governed (among other factors) by temperature. The effect was significant for all measurements (129 units) however not on the subcategory of water-measurements (45 units). The E_{pit}-values are in expected order. It might however be that the measurement done at 30 °C suffered crevice corrosion as opposed to pitting corrosion, indicated by the less rapid increase of current [1]. The order of E_{corr} is governed by temperature although an effect of dissolved oxygen could be present.

With the effects noted and the sensitivity of the method confirmed as presented in this section the inhibitory action of SS 316L in presence of dairy can be evaluated in the next section.

4.2.2 Inhibition in dairy solutions

The presence of milk powder in the electrolyte at various concentrations exhibited significant inhibitory effects on the pitting corrosion of SS 316L. Based on 113 measurements the pitting occurred at more noble potentials when the electrolyte contained dairy across all temperatures and salt concentrations. No significant differences on OCP & E_{corr} was noted due to varying milk concentrations. However variation between measurements occurred.

The inhibitory effect can indicate that the food processing equipment could be used for a longer time period or during more harsh processing conditions than expected when processing dairy solutions as compared to the reference (no milk). Although as mentioned in section 2.5 other problems are associated with processing of dairy products such as fouling and biofilms which can induce pitting. An example of CPDP curves with varying milk concentrations is presented in figure 19.

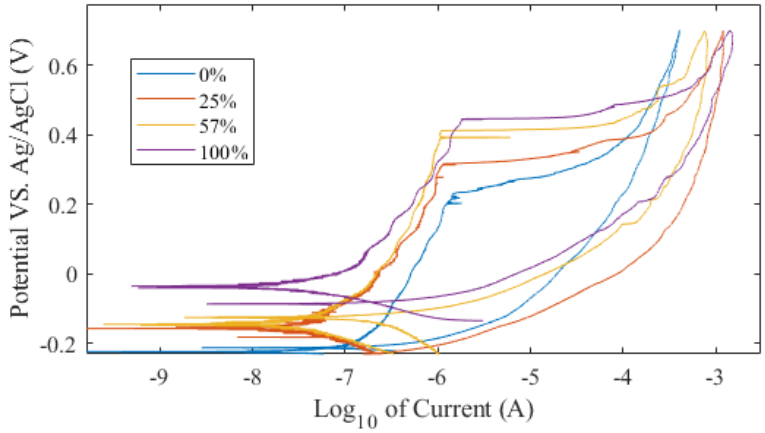

Figure 19: Varying milk concentrations for 1000 ppm at 60 °C. The highest pitting potential is for 96 g/950 mL (100 %), with decreasing milk content resulting in a subsequently lower pitting potential. Corrosion potential is ordered in the same order.

The most noble (high) E_{pit} is for the solution containing the highest amount of dairy. The E_{corr} in this case decreases with decreasing dairy concentration. The difference $E_{pit} - E_{corr}$ is similar across the varying milk concentrations. The size of the hysteresis is larger for the solutions containing milk, which indicate that the metal surface could have experienced more damage with milk present even when the pitting onset occurs during higher applied potentials. It could also be an effect of under deposit crevice corrosion occurring as an increase of milk in solution often resulted in accumulation on the sample surface, which is discussed further in section 4.3.

The inhibitory effect varied across the tested parameter sets. See figure 20 for scatter plots of the pitting potential for the different salt concentrations at 30 °C. For full dosage of milk (96 g powder/950 mL water) the pattern of inhibition (increasing E_{pit}) is more clear compared to for the other concentrations. Both 55 g and 24 g have E_{pit}-values with and without milk that are similar or lower than in non-milk solutions.

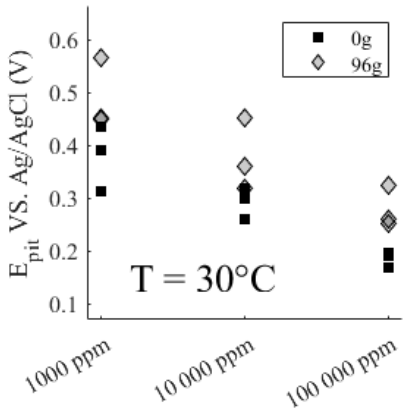

(a) Pitting potentials for 100 % milk.

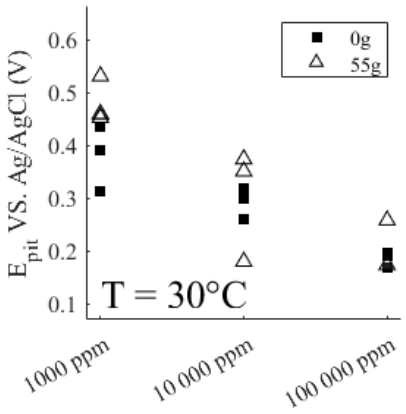

(b) Pitting potentials for 57 % milk.

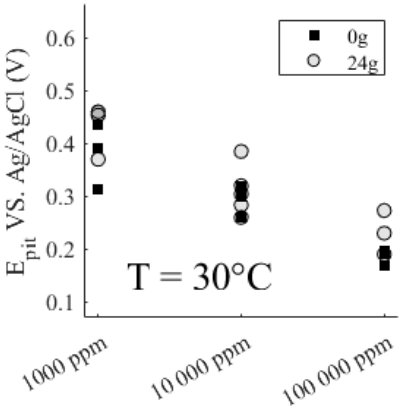

(c) Pitting potentials for 25 % milk.

Figure 20: Scatter plots for all measurements at 1000 ppm, 10 000 ppm and 100 000 ppm containing milk and no milk at 30 °C.

A summary of the mean pitting potentials observed at 30 °C can be seen in figure 21 with trend lines between each mean value. In line with the scatter plots 96 g increases the E_{pit}-value the most while the other concentrations are more similar to the reference value.

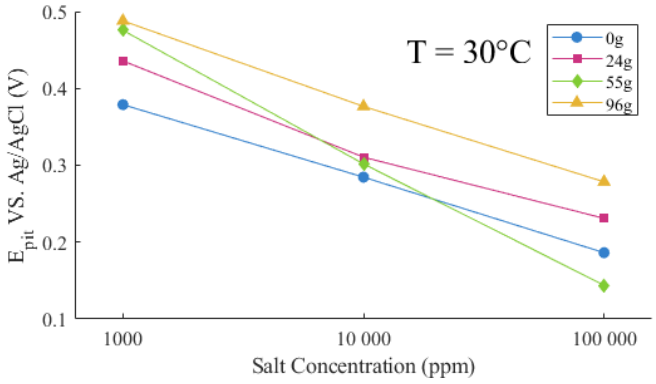

Figure 21: Mean values of the pitting potential for varying salt and milk concentrations at 30 °C.

Similar observations were made at 60 °C and the biggest inhibitory effect seems to be for 96 g see

figure 22. The inhibitory effect seems to be smaller with increasing salt in general and decreasing milk concentration. This can be interpreted as the smaller difference in pitting potential occurring for example between 1000 ppm and 100 000 ppm in 22b and in 22c.

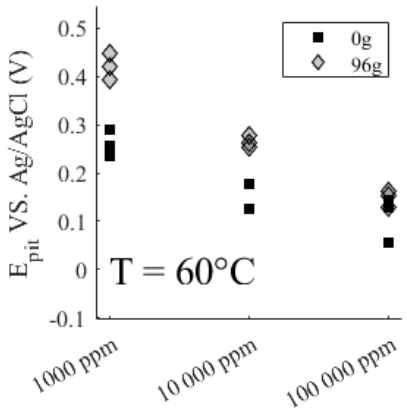

(a) Pitting potentials for 100 % milk.

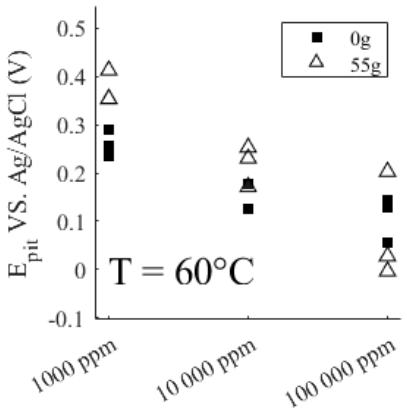

(b) Pitting potentials for 57 % milk.

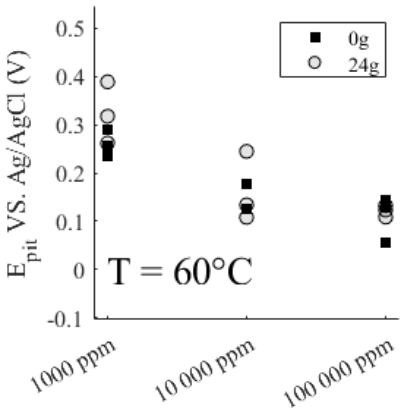

(c) Pitting potentials for 25 % milk.

Figure 22: Scatter plots for all measurements at 1000 ppm, 10 000 ppm and 100 000 ppm containing milk and no milk at 60 °C.

A summary of the mean pitting potentials observed at 60 °C can be seen in figure 23 with trend lines between each mean value. In line with the scatter plots 96 g increases the E_{pit}-value the most.

The E_{pit}-values measured at 80 °C can be seen in figure 24. Compared to the other temperatures the lower concentrations of milk (24 g and 55 g) seems to perform better at 80 °C, since most measurements are above the reference values ((0 g). The effect is seemingly not as prevalent at 100 000 ppm for all milk concentrations. The biggest increase of E_{pit} across all measurements based on mean values was 0.21V and was for 80 °C, 55 g/950 mL and 1000 ppm. That equals an inhibitory effect of 178%. See figure 25 for mean values plotted with trend-lines for measurements at 80 °C.

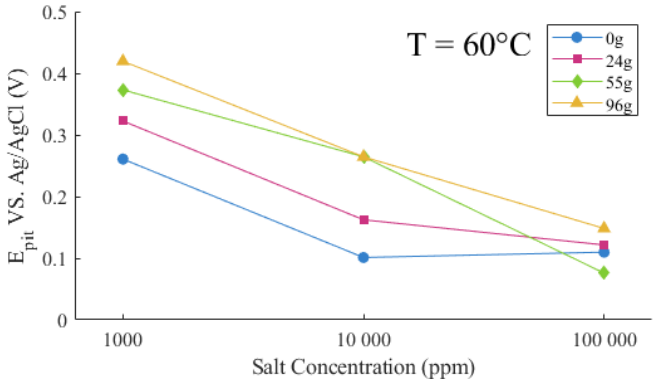

Figure 23: Mean values of the pitting potential for varying salt and milk concentrations at 60 °C.

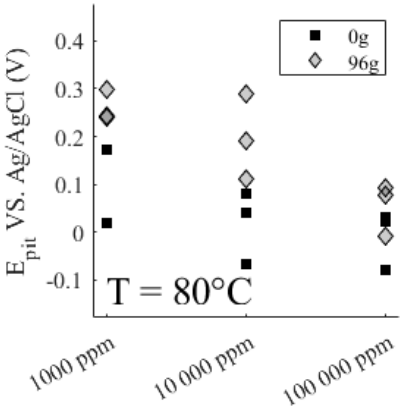

(a) Pitting potentials for 100 % milk..

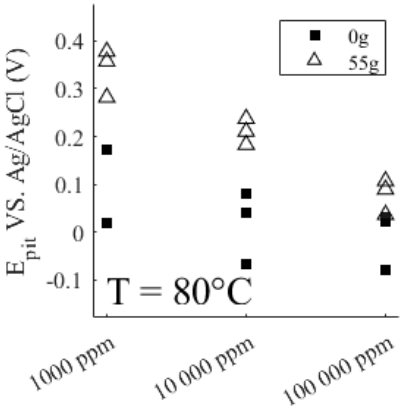

(b) Pitting potentials for 57 % milk.

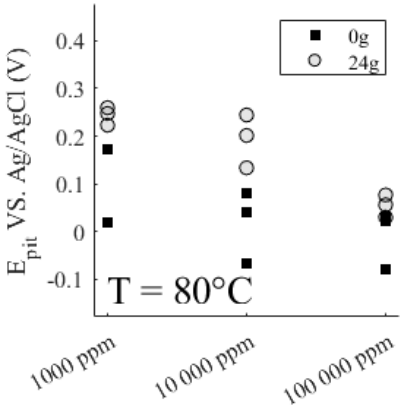

(c) Pitting potentials for 25 % milk.

Figure 24: Scatter plots for all measurements at 1000 ppm, 10 000 ppm and 100 000 ppm containing milk and no milk at 80 °C.

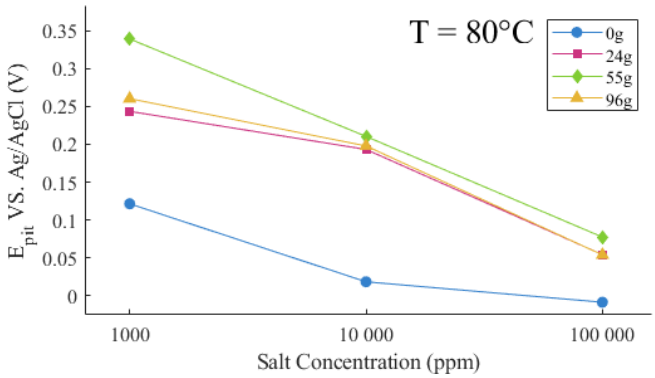

Figure 25: Mean values of the pitting potential for varying salt and milk concentrations at 80 °C.

The inhibitory effects hinted at in the scatter plots was significant at the confidence level $\alpha = 0.05$. The differences in significance was assessed with a post-hoc test and all measurements including milk (salt concentrations 1000 ppm, 10 000 ppm, 100 000 ppm, all temperatures) exhibited a difference between no milk and milk containing solutions. 57 % milk was not different from either 100 % or 25 %. However 100 % milk was different from 25 %. See figure 26 for post-hoc results of the milk inhibitory affect across all temperatures and salt concentrations. The population marginal mean (PMM) is an adjusted mean where effects can be filtered by removing effects by chosen variables.

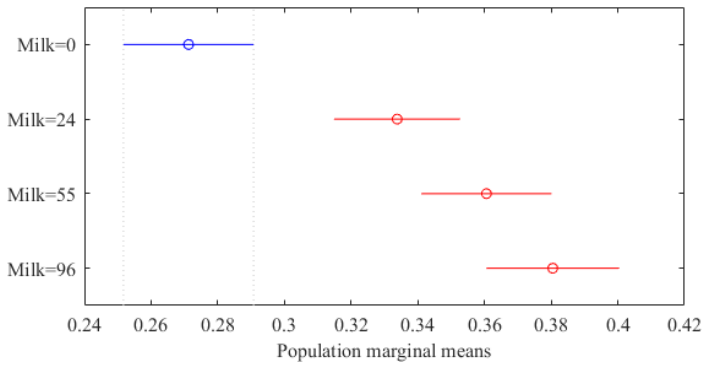

Figure 26: Post-hoc test for measurements at salt levels 1000 ppm, 10 000 ppm, 100 000 ppm and all temperatures. Significant difference exists between 100 % and (0 % and between 100 % and 25 %.

The size of the differences varied across temperature and salt concentrations. See figure 27 for a post-hoc test comparing significance induced by varying salt concentrations.

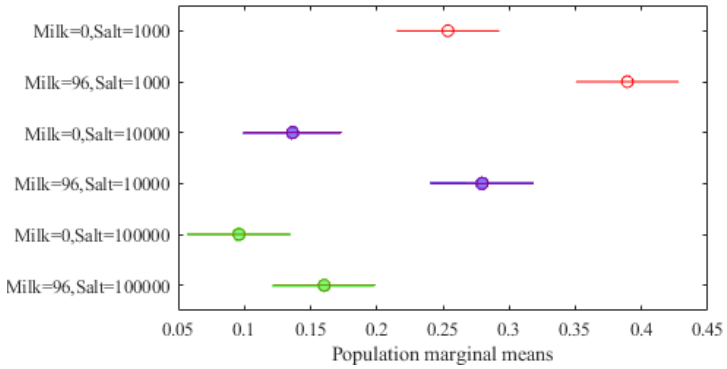

Figure 27: Population marginal means based on salt concentration. The inhibitory effect, ie. difference of population marginal means between (0 % and 100 % milk concentration is similar for 1000 ppm and 10 00ppm and 100 000 ppm differs from the former. No difference exists for 100 % milk at 10 000 ppm and (0 % milk at 1000 ppm and for 100 % milk at 100 000 ppm and (0 % milk at 10 000 ppm.

An inhibitory effect was found when comparing (0 % and 100 % for the salt concentrations 1000 ppm and 10 000 ppm. However there was no difference in pitting potentials for 100 000 ppm of salt. The effect was also present when comparing based on the difference of $E_{pit} - E_{corr}$. This indicates that the inhibitory mechanism occurring for the other salt concentrations could be limited at high salt concentrations. Since there is no difference for 1000 ppm without milk and 10 000 ppm with milk, these two concentrations of salt could potentially be processed with equipment of the same steel grade and exhibit similar pitting patterns, even though the chloride concentration is ten times larger in the later. The same comparison could be made for 10 000 ppm without milk and 100 000 ppm with milk. These observations hint at that 100 % milk inhibits a ten-fold increase of salt in the experimental setup. The results should be translated to reality with caution. The lack of the inhibitory effect during higher salt concentrations could be due to many factors. Increasing the ionic species would result in a higher conductivity in the solution [54], more chloride ions at the surface inducing pitting corrosion [2] and a change in casein solubility and increase of viscosity [57], all of which could lead to a reduction of inhibitory effects. An increase of chloride ions could also compete for adsorbing sites with a potential inhibitory compound present in the milk, in similarity to the discussed inhibitors in section 2.4.2.

There was a difference of pitting potential across all temperatures, with a similar inhibitory effect by dairy being induced at each level when comparing (0 % and 100 % milk. See figure 28 for E_{pit} population marginal means variation due to milk concentration and temperature.

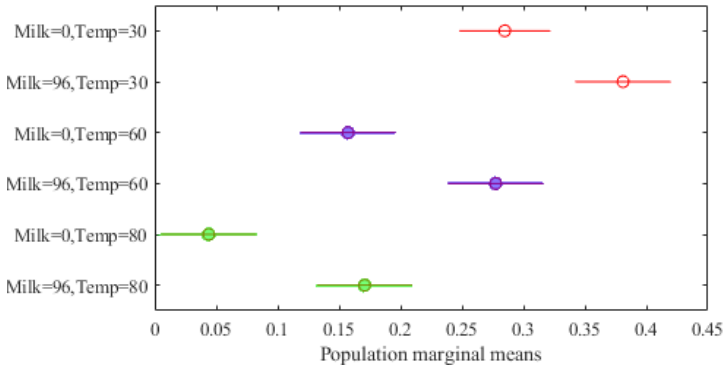

Figure 28: Population marginal means based on temperature. The inhibitory effect, ie. difference of population marginal means between (0 % and 100 % milk concentration is similar across temperatures. No difference exists for 100 % milk at 60 °C and (0 % milk at 30 °C and for 100 % milk at 80 °C and (0 % milk at 60 °C.

Similar pitting potential is obtained without milk at 30C and with milk at 60 °C. The same can be noted for without milk at 60 °C and with milk at 80 °C. This indicates that milk inhibits the susceptibility to pitting corrosion otherwise observable when increasing the temperature. During this experiment the inhibitory effect can be quantified to counter a temperature increase of around 20-30 °C. This indicates that SS 316L could be suitable for processing of for example water at 30 °C and 100 % dairy at 60 °C if either does not perform bad in terms of pitting corrosion when used in food processing equipment.

The biggest measured inhibitory effect (significant difference on E_{pit} population marginal means, α = 0.05), was for the salt concentration 10 000pm. The difference was 0.143 V, the other differences are reported in Table 5.

Table 5: Difference in Population marginal means of E_{pit}, temperature and salt concentration for (0 % vs. 100 % milk concentration. All differences are significant (α = 0.05) except for 100 000 ppm.

Parameter	**Mean difference for 0% and 100% milk content (V)**
1000 ppm	0.135
10 000 ppm	0.143
100 000 ppm	0.064
30 °C	0.096
60 °C	0.120
80 °C	0.126

The smallest inhibitory effect was at the highest salt concentration (100 000 ppm), where no difference was found. This is probably due to the increase of driving force towards pitting corrosion with an increase of salt concentration [2]. The inhibitory effect is similar for salt concentrations 1000 ppm and 10 000 ppm. The smallest inhibitory effect based on temperature is for 30 °C. This could be that proteins associate to the surface [60] [61] more efficiently during higher temperatures, ie. cause fouling. This is supported by the general fouling behaviour by proteins as noticed in food processing during heating operations [63]. However fouling and protein association is also dependent on species present and more

unfolded and native structures will decrease the amount of fouling [71], which also could contribute to the effect. More fouling was noted for the higher temperatures which likely affects the inhibitory mechanism. This could be a reason for the slight differences between the scatter plots in figures 20, 22 and 24 and the differences in significant effect as reported in the table above. As presented in section 2.4.2, inhibition of SS 316L has previously been reported to be by adsorption of compounds containing an excess of electrons (pi-bond, heteroatoms, aromaticity), which likely contributes to the inhibitory effect exhibited in this report. It could be different molecules being effective inhibitors at different temperatures and during different salt concentrations.

No differences by milk when analyzing the polarization resistance (R_p) was found in proximity of E_{corr}. This could be due to that the OCP/E_{corr} values as mentioned were difficult to stabilize and not always similar during OCP and CPDP-measurements. This could have been due to the dynamic surface and non-static conditions. The significant difference based on (R_p) was for 30 °C and 80 °C. The R_p was for samples at 80 °C lower than for 30 °C, however no difference was exhibited between either 30 °C and 60 °C or 60 °C and 80 °C. Which could be due to ionic movement increasing or that the oxide layer is less resistant to polarization at higher temperatures. To utilize R_p as another parameter to evaluate inhibition the OCP-values should be measured for an extended period of time for an indication of the time required for stability of oxide and electrolyte interactions.

4.3 Evaluation of method using dairy products as electrolyte

The method has previously exhibited good results when used to evaluate pitting corrosion of SS by temperature and salt concentrations during simulated food processing conditions [10]. The change to the sample preparation routine, using a holder and only grinding with SiC 220, (from [10] and [31]) also allowed for production of significant results. The method sensitivity, accuracy and robustness is however probably affected when altering the recommended grinding [31].

The method yielded a mixture of results. Although a majority of measurements resulted in sharp current increases typical for pitting corrosion and significant differences could be distinguished some measurements resulted in curves more similar to crevice corrosion. For example in figure 18 the curve obtained at 30 °C exhibits a less instant increase of current, which indicate crevice corrosion [10]. This can be contributed in part to the parameters used during measurements and in part to the inevitable crevice corrosion occurring to varying degree at the O-ring. At lower temperatures and salt concentrations high potentials could be reached without pitting current increase. Crevice corrosion requires a higher applied potential (in combination with stagnancy) to be initiated. It is also likely that the first corrosion to be initiated on the surface was pitting and that in some cases crevice corrosion followed during higher potentials. Another source of crevice corrosion could be the under deposit crevices created by stagnant milk on the sample surface. See figure 29 for examples of milk residue on the sample surface.

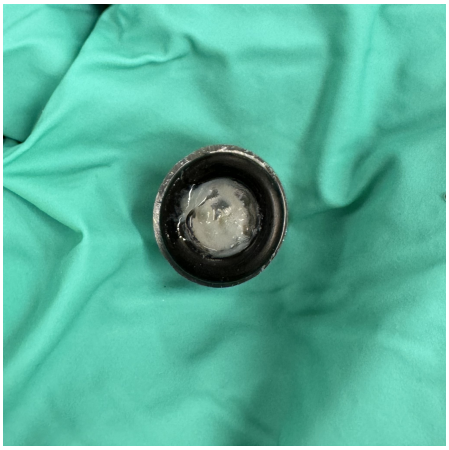


Figure 29: Fouled samples, *left* from processing at 1000 ppm, 30 °C and 96 g/950 mL milk and *right* from 1000 ppm, 80 °C and 96 g/950 mL.

Notably during higher temperatures the milk often became discolored at the sample surface. No discoloration of the electrolyte in liquid form was however evident. A lower flow-rate in the corrosion testing machine was tested initially with the pre-set flow (15 Hz) and the milk residue was more prevalent on the sample surface. This setting was quickly changed to the used 30 Hz to combat the product build-up. Increasing it further could be a good idea to increase the turbulence and alter the flow profile in the test chamber. There could also be interactions occurring between molecules in the milk and the sample surface, as previously reported [60] [61]. This accumulation was less prevalent in presence of high salt content and during lower temperatures and lower milk concentrations. This is in line with the viscosity increase occurring during higher temperatures [54]. The accumulation of milk species likely contributes to OCP and E_{corr}-variations, as the surface conditions are not static with residue likely accumulating and detaching during the OCP and CPDP-measurements.

The cyclic polarization cutoff should probably be decreased to allow for repassivation. The cutoff was based on ASTM standard [31] however there is likely a substantial current loss from the sample surface to the potentiostat. In the presented CPDP graphs a cutoff close to 0.1 mA would be a good choice, as compared to the utilized 1.9 mA. The potentials reached to obtain the cutoff is for some measurements above 0.7 olt vs Ag/AgCl and as mentioned at 0.8 V vs Ag/AgCl the oxygen evolution potential is obtained which likely is of no interest in food processing applications. Less crevice corrosion might be induced if the cutoff and reversal occurs closer to the rapid current increase characteristic of pitting corrosion.

The cooling effect obtained during the experiments could be improved as operating temperatures 30 °C, 60 °C and 80 °C only was cooled to 25 °C, 40 °C and 50 °C respectively. This is not equal to as if new product was circulated in the system, defeating the purpose somewhat. However it is preferential to keeping milk at for example 80 °C degrees for extended time periods. The cooling effect could be improved by using fresh tap water.

4.3.1 Measurement precision

The precision of the measurements varied with the three replicates of each parameter set, see example of three replicates in figure 30. Potential factors resulting in error could be contamination by previous experiment. Pitting corrosion is highly surface dependent, and the amount of MnS inclusions and differences in surface morphology where the passive film might be more susceptible to penetration/breakage

or simply not regenerate sufficiently enough likely varied throughout the experiments. The mean standard deviations of E_{pit} was of the three replicates was 4.75%, with no deviatons being above 8%. The mean standard deviation of E_{corr} was 8.04%, with the highest deviation being 20%. Given the stochastic nature of pitting corrosion the values of E_{pit} is expected to vary [27] and the data is likely sufficiently precise to be utilized and compared to real life pitting corrosion in service equipment, as indicated by the significance levels exhibited in previous sections. E_{corr} is not a stochastic variable and the precision of these measurements and OCP-values could probably be improved significantly by increasing the OCP-measurement time and altering the scanning rate during the CPDP could also likely affect the E_{corr}.

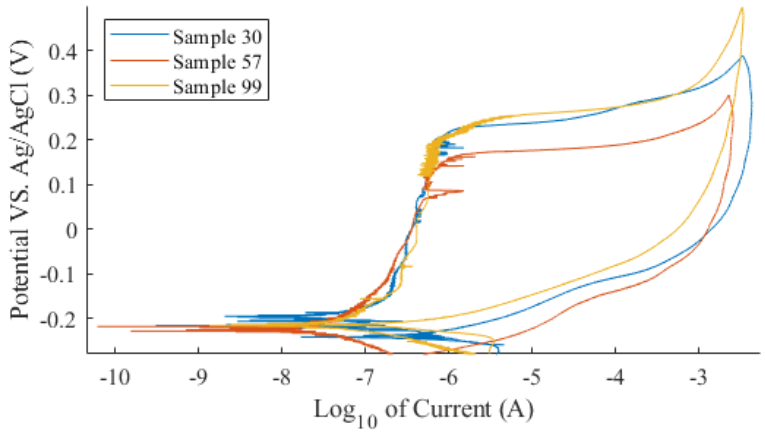

Figure 30: Three replicates for 55 g/950 mL milk, 60 °C and 10 000 ppm of salt.

5 Conclusions

The main conclusions that can be drawn from this report is that dairy inhibits pitting corrosion of SS 316L during food processing conditions as shown by analysis of data obtained from the corrosion testing setup. Tetra Pak can use both the data and method as assistance in corrosion risk evaluations. Previously reported mechanisms of inhibition by electron rich molecules or protein deposition (fouling) could have been the cause of inhibition for SS 316L in dairy solutions. However to fully understand the oxide layer dynamics and inhibition the employed method could be supplemented with additional analytical techniques if it is of interest to Tetra Pak.

Many factors affect the method and localized corrosion as reported in the literature review and an absolute understanding is probably not required to *utilize* the method in material selection of food processing equipment. Comparing pitting corrosion onset and parameters could provide insight into which processing combinations that could be processed in similar equipment. Especially comparing the experimental corrosion parameters to real-life pitting corrosion in food processing environments could aid in material selection for novel food products for which the industry lack specific experience. The kinetics of applied potential and obtained E_{pit} values has to be translated to time and temperatures during processing to predict corrosion and utilize the data on its own for material selection. Suggested improvements to the electrochemical measurements is to alter the scan rate, cutoff and time of measurement. To potentially look at inhibition close to the OCP and E_{corr}-value using R_p it would be beneficial to include longer OCP-measurements to get an indication of how long time the oxide layer requires for stability. This would also be beneficial since the OCP and E_{corr} did not always align.

It would be interesting to look at the hysteresis and metastable-pitting using statistical methods to see if these are affected in the presence of milk. The most important parameter to evaluate pitting corrosion is E_{pit}, however evaluating hysteresis and metastable-pitting could potentially aid Tetra Pak in obtaining a more complete image of the problem.

The adjustment of grinding with 220 SiC-paper to suit food processing standard (0.7 µm) likely resulted in a loss in precision and the results were not always in expected order. Crevice corrosion should be eliminated and the flow profile in the test chamber should be altered to limit food deposit on the sample surface. A more turbulent flow would likely aid to reduce the crevice corrosion occuring. The flow rate and profile could also be varied as an experimental parameter to get an indication of how flow can be altered to limit pitting corrosion in food processing equipment.

Incorporating the changes proposed to the method will enhance the reliability of the corrosion parameters to guide in material selection, in order to ensure safety and longevity of the of food processing equipment while not using resources in unsustainable ways and over-engineering components.

6 Outlook

- **Reversal of scanning direction in NOVA** should be decreased from the ASTM standard [31]. This due to the rust occurring on the screw fastening it, as this would make the apparent current lower than the real current. The best way to alter the cutoff would be by comparing when the curve should be reversed from a few graphs. From the graphs presented in this section a cutoff matching 0.1mA would probably be more suitable than 1.9mA. The current should also be altered based on the changes occurring during applying pressure to the O-ring since the exposed area of the sample is *not* the same as the area of the O-ring in its relaxed state.

- **The cooling effect** should be increased especially to eventually heat electrolytes to 140°C. In experiments at 30 °C the recirculated stream went down to around 25°C, 60 °C went down to 40°C and 80 °C to (50 °C. Decreasing the temperatures by more efficient cooling could counteract the accumulation of milk product and the experimental conditions would be more similar to real life processing conditions where new product is pumped through the system.

- **OCP** measurements could be done for a longer time during flow to get an indication of OCP-evolution and attempt to match the E_{corr} and OCP better. This to potentially utilize the R_p to look at inhibition close to the OCP-value. It would also be of interest to conduct longer OCP measurements before cyclic polarization to determine if there is differences in pitting behaviour based on immersion time, as this could be used in industry in terms of recommending operating times.

- **Surface analysis by microscopy** should be considered to look at extent of pitting and where it occurs. SEM and XPS could be beneficial to look for structures and changes in composition on surface as induced by electrochemical measurements. However the grinding to suit SEM is usually below finer than by SiC 200 roughness, which has to be taken into account.

- **Flow-profile** should be altered, easily by increasing the flow rate but changes to chamber could also be beneficial. This to limit crevice corrosion induced under deposits of electrolyte that foules the surface and potentially by the O-ring.

- **Match applied potential to simulations/industry data** to utilize the potentials that induce pitting and match that to pitting during processing conditions. Energy supplied at the surface by applied potential could potentially be matched to the energy required to induce pitting over time by comparing it to simulations or real data of pitting in food processing equipment.

- **Utilizing the dairy database to find inhibitory compounds** to determine which species might be adsorbing on the surface and/or inhibiting the corrosion on SS 316L. A method to do this could be: 1. Filter the database for compounds containing a) π-bonds b) aromaticitiy c) hetero atoms 2. Looking at concentrations of inhibitory studies (mol/cm2 of SS-sample) 3. Filter the database for species at sufficient concentration 4. Conduct simulations to see how the energy of adsorption vary between a few likely compounds. Following this chemical analysis and testing with the corrosion testing machine (Sören) with additions of potential inhibitors could be initiated.

- **Asses flow rate effects on inhibition** to fully utilize the capacities of the corrosion testnig machine different flow rates should be assessed. Different Re-numbers has been reported to induce differences in the electrical double layer, which could effect the oxide layer interface and thus the oxide layer evolution/stability.

- **Test other food products** such as juices, fattier milk products, plant based products and/or products with viscosity changes due to flow and/or temperature.
- **Utilize complementary electrochemical & analytical techniques** per example EIS (Electrochemical Impedence Spectroscopy) to gain an understanding of the oxide layer and how it is altered during varying process parameters. In most reports on inhibition and corrosion a combination of techniques are used to deduct and confirm results.
- **Data evaluation** should include size and degree of hysteresis and not just be done by visual inspection. Either by integration or scanning the CPDP curves for largest current variation at same potential. This would require adjustment to the CPDP routine first. The data analysis could also include more statistical techniques such as PCA and PLS.

References

[1] E Mccafferty. *Introduction to Corrosion Science*. Springer Science-, London, 2010.

[2] H. Boehni. Pitting and crevice corrosion. In *Brown Boveri Symposia Series*, pages 29–52. Plenum Press, 1984.

[3] Rongxuan Zhao, Qian Yu, and Lin Niu. Corrosion inhibition of amino acids for 316L stainless steel and synergistic effect of I ions: Experimental and theoretical studies. *Materials and Corrosion*, 73(1):31–44, 1 2022.

[4] Tibnor. Rostfritt stål: Teknisk Data, 2024.

[5] Abdulaziz Alhazaa and Nils Haneklaus. Diffusion bonding and transient liquid phase (TLP) bonding of type 304 and 316 austenitic stainless steel—A review of similar and dissimilar material joints, 5 2020.

[6] P F Fox, T Uniacke-Lowe, P L H Mcsweeney, and J A O'mahony. *Dairy Chemistry and Biochemistry Second Edition*. Springer, second edition edition, 2015.

[7] Michiel van Dijk, Tom Morley, Marie Luise Rau, and Yashar Saghai. A meta-analysis of projected global food demand and population at risk of hunger for the period 2010–2050. *Nature Food*, 2(7):494–501, 7 2021.

[8] Elahe Shekari, Faisal Khan, and Salim Ahmed. Economic risk analysis of pitting corrosion in process facilities. *International Journal of Pressure Vessels and Piping*, 157:51–62, 11 2017.

[9] Branko N. Popov. Corrosion Inhibitors. In *Corrosion Engineering*, pages 581–597. Elsevier, 2015.

[10] Fredrik Waldur. Effects of Food Processing Conditions on Local Corrosion of 316L Stainless Steel, 2022.

[11] Branko N. Popov. Evaluation of Corrosion. In *Corrosion Engineering*, pages 1–28. Elsevier, 2015.

[12] Branko N. Popov. Basics of Corrosion Measurements. In *Corrosion Engineering*, pages 181–237. Elsevier, 2015.

[13] K. Cronin and R. Cocker. Materials and Finishes for Plant and Equipment. *Encyclopedia of Dairy Sciences*, pages 134–138, 12 2011.

[14] Talha Qasim Ansari, Zhihua Xiao, Shenyang Hu, Yulan Li, Jing Li Luo, and San Qiang Shi. Phase-field model of pitting corrosion kinetics in metallic materials. *npj Computational Materials*, 4(1), 12 2018.

[15] GS Frankel and N Sridhar. Understanding localized corrosion. *Materials today*, 11(10):38, 10 2008.

[16] Toshiaki Ohtsuka, Atsushi Nishikata, Masatoshi Sakairi, and Koji Fushimi. *Electrochemistry for Corrosion Fundamentals*. Springer, Singapore, 2018.

[17] Slobodan Petrovic. *Electrochemistry Crash Course for Engineers*. Springer Nature Switzerland, 2021.

[18] Gaius Debi Eyu, Geoffrey Will, Willem Dekkers, and Jennifer MacLeod. Effect of dissolved oxygen and immersion time on the corrosion behaviour of mild steel in bicarbonate/chloride solution. *Materials*, 9(9), 9 2016.

[19] Roland Tolulope Loto. Pitting Corrosion Resistance and Inhibition of Lean Austenitic Stainless Steel Alloys. In *Austenitic Stainless Steels - New Aspects*. InTech, 12 2017.

[20] S. Choudhary, R.G. Kelly, and N. Birbilis. On the origin of passive film breakdown and metastable pitting for stainless steel 316L. *Corrosion Science*, 230:111911, 4 2024.

[21] William S. Tait. Controlling corrosion of chemical processing equipment. In *Handbook of Environmental Degradation Of Materials: Third Edition*, pages 583–600. Elsevier Inc., 6 2018.

[22] RG Kelly and JS Lee. Localized Corrosion: Crevice Corrosion. *Electrochemical Techniques in Corrosion Science and Engineering*, pages 292–301, 2018.

[23] A. M. Taher. Evaluating corrosion and passivation by using electrochemical techniques. *International Journal of Mechanical Engineering and Robotics Research*, 7(2):131–135, 3 2018.

[24] R. Ghamsarizade, Bahram Ramezanzadeh, and H. Eivaz Mohammadloo. Corrosion measurements in coatings and paintings. In *Electrochemical and Analytical Techniques for Sustainable Corrosion Monitoring: Advances, Challenges and Opportunities*, pages 217–264. Elsevier, 1 2023.

[25] X. L. Zhang, Zh H. Jiang, Zh P. Yao, Y. Song, and Zh D. Wu. Effects of scan rate on the potentiodynamic polarization curve obtained to determine the Tafel slopes and corrosion current density. *Corrosion Science*, 51(3):581–587, 3 2009.

[26] Qingqing Sun and Kanghua Chen. Potential difference of cyclic polarization curve of an aircraft al alloy. *Journal of Electrochemical Science and Technology*, 11(2):140–147, 2020.

[27] Neusa Alonso-Falleiros and Stephan Wolynec. Correlation between Corrosion Potential and Pitting Potential for AISI 304L Austenitic Stainless Steel in 3.5% NaCl Aqueous Solution. *Materials Research*, 5(1):7784, 2002.

[28] Haixian Liu, Jiaqi He, Zhengyu Jin, and Hongwei Liu. Pitting corrosion behavior and mechanism of 316L stainless steel induced by marine fungal extracellular polymeric substances. *Corrosion Science*, 224, 11 2023.

[29] Masoud Atapour, Zheng Wei, Himanshu Chaudhary, Christofer Lendel, Inger Odnevall Wallinder, and Yolanda Hedberg. Metal release from stainless steel 316L in whey protein - And simulated milk solutions under static and stirring conditions. *Food Control*, 101:163–172, 7 2019.

[30] A. Szewczyk-Nykiel, M. Skałoń, and J. Kazior. Corrosion behaviour of sintered AISI 316L stainless steel modified with boron-rich master alloy in 0.5m NaCl water solution. *Archives of Metallurgy and Materials*, 60(3A):1795–1800, 2015.

[31] Standard Test Method for Conducting Cyclic Potentiodynamic Polarization Measurements for Localized Corrosion Susceptibility of Iron-, Nickel-, or Cobalt-Based Alloys 1. Technical report.

[32] S. H. Mameng, R. Pettersson, and J. Y. Jonson. Limiting conditions for pitting corrosion of stainless steel EN 1.4404 (316L) in terms of temperature, potential and chloride concentration. *Materials and Corrosion*, 68(3):272–283, 3 2017.

[33] S. Esmailzadeh, M. Aliofkhazraei, and H. Sarlak. Interpretation of Cyclic Potentiodynamic Polarization Test Results for Study of Corrosion Behavior of Metals: A Review. *Protection of Metals and Physical Chemistry of Surfaces*, 54(5):976–989, 9 2018.

[34] B. Zhang and X. L. Ma. A review—Pitting corrosion initiation investigated by TEM, 7 2019.

[35] Jiabin Han, Yang Yang, Srdjan Nesic, and Bruce N Brown. Roles of Passivation and Galvanic Effects in Localized CO2 Corrosion of Mild Steel. In *NACE International Conference and Expo*, 2008.

[36] N. Anita, R. M. Joany, R. Dorothy, Jeenat Aslam, Susai Rajendran, A. Subramania, Gurmeet Singh, and Chandrabhan Verma. Linear polarization resistance (LPR) technique for corrosion measurements. In *Electrochemical and Analytical Techniques for Sustainable Corrosion Monitoring: Advances, Challenges and Opportunities*, pages 59–80. Elsevier, 1 2023.

[37] Lakshmanan Muthulakshmi, G. Seghal Kiran, Seeram Ramakrishna, Kai Y. Cheng, Remya Ampadi Ramachandran, Mathew T. Mathew, and Catalin I. Pruncu. Towards improving the corrosion resistance using a novel eco-friendly bioflocculant polymer produced from Bacillus sp. *Materials Today Communications*, 35, 6 2023.

[38] Temitope Olumide Olugbade. Corrosion Resistance, Evaluation Methods, and Surface Treatments of Stainless Steels. *Intech Open*, 2022.

[39] Sandmeyer Steel. Specification Sheet: Alloy 316/316L (UNSS31600, S31603), 2024.

[40] Zuocheng Wang, Antoine Seyeux, Sandrine Zanna, Vincent Maurice, and Philippe Marcus. Chloride-induced alterations of the passive film on 316L stainless steel and blocking effect of prepassivation. *Electrochimica Acta*, 329, 1 2020.

[41] Wen-Ta Tsai, Ying-Nan Wen, Ju-Tung Lee, and Hon-Yee Liou. EFFECT OF SILICON ADDITION ON THE MICROSTRUCTURE AND CORROSION BEHAVIOR OF SINTERED STAINLESS STEEL. *Surface and Coatings Technology*, 34:209–217, 1988.

[42] Rock-Hoon Jung, Hiroaki Tsuchiya, and Shinji Fujimoto. Growth Process of Passive Films on Austenitic Stainless Steels under Wet-dry Cyclic Condition. *ISIJ International*, 52(7):1356–1361, 2012.

[43] Ying Ren, Yuchen Li, Jun Shen, Shaojun Wu, Liting Liu, and Genshu Zhou. Revealing the Corrosion Resistance of 316 L Stainless Steel by an In Situ Grown Nano Oxide Film. *Nanomaterials*, 13(3), 2 2023.

[44] P J Potts. X-Ray Fluorescence and Emission, 2005.

[45] Scott A. Elias. Geoarchaeology. In *Encyclopedia of Geology: Volume 1-6, Second Edition*, volume 6, pages 538–553. Elsevier, 1 2020.

[46] Sergio Musazzi and Umberto Perini. Laser-Induced Breakdown Spectroscopy: Theory and Applications. In *Springer Series in Optical Sciences*, volume 182. Springer, Berlin, 2014.

[47] Mustapha Alahiane, Rachid Oukhrib, Youssef Ait Albrimi, Hicham Abou Oualid, Rachid Idouhli, Ayssar Nahlé, Avni Berisha, Nizar Z. Azzallou, and Mohamed Hamdani. Corrosion inhibition of SS 316L by organic compounds: Experimental, molecular dynamics, and conceptualization of molecules–surface bonding in H2SO4 solution. *Applied Surface Science*, 612, 3 2023.

[48] Jeanette Karlsson. Pitting corrosion on stainless steel with and without passivation, 2017.

[49] Aidin Foroutan, An Chi Guo, Rosa Vazquez-Fresno, Matthias Lipfert, Lun Zhang, Jiamin Zheng, Hasan Badran, Zachary Budinski, Rupasri Mandal, Burim N. Ametaj, and David S. Wishart. Chemical Composition of Commercial Cow's Milk. *Journal of Agricultural and Food Chemistry*, 67(17):4897–4914, 5 2019.

[50] Mustapha Alahiane, Rachid Oukhrib, Youssef Ait Albrimi, Hicham Abou Oualid, Rachid Idouhli, Ayssar Nahlé, Avni Berisha, Nizar Z. Azzallou, and Mohamed Hamdani. Corrosion inhibition of SS 316L by organic compounds: Experimental, molecular dynamics, and conceptualization of molecules–surface bonding in H2SO4 solution. *Applied Surface Science*, 612, 3 2023.

[51] O. Sanni, A. P.I. Popoola, and O. S.I. Fayomi. Corrosion Inhibition Comparison of the Effect of Green Inhibitor on the Corrosion Behavior of 316L and 904L Austenitic Stainless Steels in Chloride Environment. In *Journal of Physics: Conference Series*, volume 1378. Institute of Physics Publishing, 12 2019.

[52] S A M Refaey, F Taha, and A M Abd El-Malak. Corrosion and Inhibition of 316L stainless steel in neutral medium by 2-Mercaptobenzimidazole. *Int. J. Electrochem. Sci*, 1:80–91, 2006.

[53] Ee Jian Low, Hanis Mohd Yusoff, Nurhanna Batar, Intan Nur Zulayqha Nor Azmi, Poh Wai Chia, Su Shiung Lam, Su Yin Kan, Rock Keey Liew, Gaik Ee Lee, Katta Venkateswarlu, and Mohammad Fakhratul Ridwan Zulkifli. The use of food additives as green and environmental-friendly anti-corrosion inhibitors for protection of metals and alloys: a review, 7 2023.

[54] Marcus Henningsson, Karin Östergren, and Petr Dejmek. The electrical conductivity of milk - The effect of dilution and temperature. *International Journal of Food Properties*, 8(1):15–22, 2005.

[55] Y. Ma and D. M. Barbano. Milk pH as a function of CO2 concentration, temperature, and pressure in a heat exchanger. *Journal of Dairy Science*, 86(12):3822–3830, 2003.

[56] Roberto Galluzzo, Valeria Damiano, Alessandro Gianfrancesco, Françoise Maynard, Rolf Meyer, Martin Michel, Annemarie Johanna Schoonman, and Rolf Jost. Milk. In *Ullmann's Encyclopedia of Industrial Chemistry*, pages 1–41. Wiley, 7 2022.

[57] Zhengtao Zhao and Milena Corredig. Changes in the physico-chemical properties of casein micelles in the presence of sodium chloride in untreated and concentrated milk protein. *Dairy Science and Technology*, 95(1):87–99, 2015.

[58] Patrícia Campos Bernardes, Emiliane Andrade Araújo, Ana Clarissa, Santos Pires, José Felício Queiroz, Fialho Júnior, Carini Aparecida Lelis, and Nélio José De Andrade. Work of Adhesion of Dairy Products on Stainless Steel Surfaces. *Brazilian Journal of Microbiology*, pages 1261–1268, 2012.

[59] Masoud Atapour, Inger Odnevall Wallinder, and Yolanda Hedberg. Stainless steel in simulated milk and whey protein solutions – Influence of grade on corrosion and metal release. *Electrochimica Acta*, 331, 1 2020.

[60] L.-M Barnes, M F Lo, M R Adams, and A H L Chamberlain. Effect of Milk Proteins on Adhesion of Bacteria to Stainless Steel Surfaces. *Applied and Enviromental Microbiology*, 65(10):4543–4548, 1999.

[61] Nguyen Manh Dat, Daisuke Hamanaka, Fumihiko Tanaka, and Toshitaka Uchino. Surface conditioning of stainless steel coupons with skim milk solutions at different pH values and its effect on bacterial adherence. *Food Control*, 21(12 SUPPL.):1769–1773, 2010.

[62] Andrea Zaffora, Francesco Di Franco, and Monica Santamaria. Corrosion of stainless steel in food and pharmaceutical industry, 10 2021.

[63] J Visser and Th J M Jeurnink. Fouling of Heat Exchangers in the Dairy Industry. *Experimental Thermal and Fluid Science*, 14(4):407–424, 5 1997.

[64] Somil Gupta and Sanjeev Anand. Induction of pitting corrosion on stainless steel (grades 304 and 316) used in dairy industry by biofilms of common sporeformers. *International Journal of Dairy Technology*, 71(2):519–531, 5 2018.

[65] Birgitte Carpentier. Biofilms. *Encyclopedia of Food Microbiology*, 1999.

[66] John Milledge. The cleanability of stainless steel used as a food contact surface: An updated short review. *Food Science and Technology*, 2010.

[67] Mary Ann Augustin. Milk Powders in the Marketplace. In *Encyclopedia of Food Sciences and Nutrition*, pages 4694–4702. Elsevier, 2003.

[68] Hu Zhou, Danny Chhin, Alban Morel, Danick Gallant, and Janine Mauzeroll. Potentiodynamic polarization curves of AA7075 at high scan rates interpreted using the high field model. *npj Materials Degradation*, 6(1), 12 2022.

[69] by Kang Hoon Choi. *Electrochemical Passivation of 316L Stainless Steel for Biomedical Applications: A Method for Improving Pitting Corrosion Resistance via Cyclic Potentiodynamic Polarization*. PhD thesis, McGill University, Montreal, 2019.

[70] Wei Xing, Min Yin, Qing Lv, Yang Hu, Changpeng Liu, and Jiujun Zhang. Oxygen Solubility, Diffusion Coefficient, and Solution Viscosity. In *Rotating Electrode Methods and Oxygen Reduction Electrocatalysts*, pages 1–31. Elsevier B.V., 2014.

[71] Olga Santos, Tommy Nylander, Karin Schillén, Marie Paulsson, and Christian Trägårdh. Effect of surface and bulk solution properties on the adsorption of whey protein onto steel surfaces at high temperature. *Journal of Food Engineering*, 73(2):174–189, 3 2006.

7 Appendix

A1 Statistical analysis of data

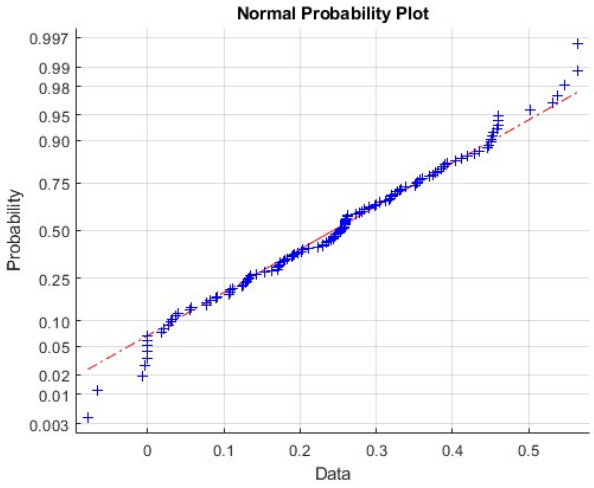


```
ans =

  logical

   0
```

Figure 31: Normplot of E_{pit}-values. The data follows a normal distribution with some values at each endpoint differing some from the normal distribution. Result of Anderson-Darling test, 0 indicates that the hypothesis of the data following a normal distribution cannot be rejected at confidence $\alpha = 0.05$.

Analysis of Variance

Source	Sum Sq.	d.f.	Mean Sq.	F	Prob>F
Temp	0.72769	2	0.36384	100.07	3.22812e-26
Salt	1.59166	4	0.39791	109.44	6.42636e-39
Milk	0.17639	3	0.0588	16.17	7.01696e-09
Error	0.43269	119	0.00364		
Total	2.75576	128			

Constrained (Type III) sums of squares.

Figure 32: ANOVA for whole sample set. All tested parameters are significantly affecting the pitting potential.

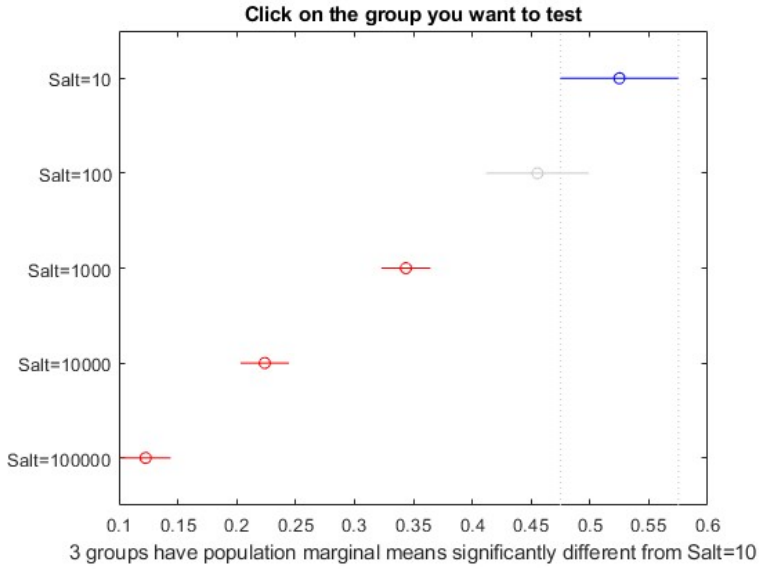

Figure 33: Post-hoc for salt. 10 ppm and 100 ppm exhibits larger bars due to fewer measurements (not tested for milk - fewer experimental units for these salt concentrations).

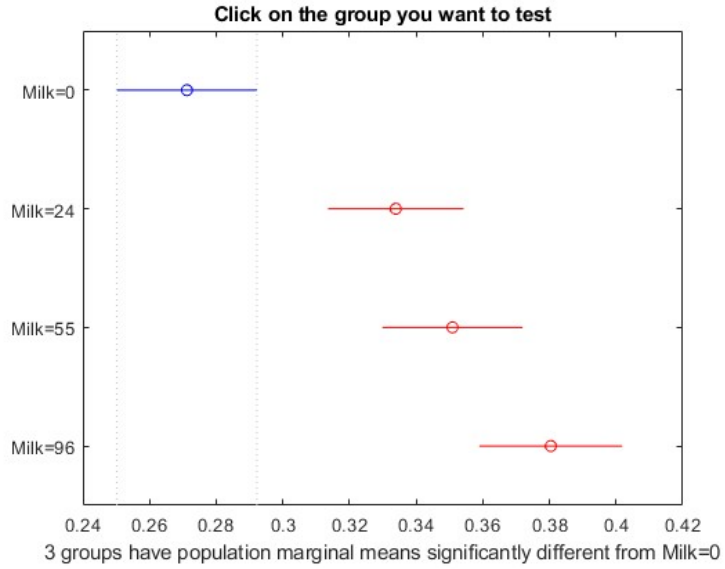

Figure 34: Post-hoc for milk, all measurements containing milk.

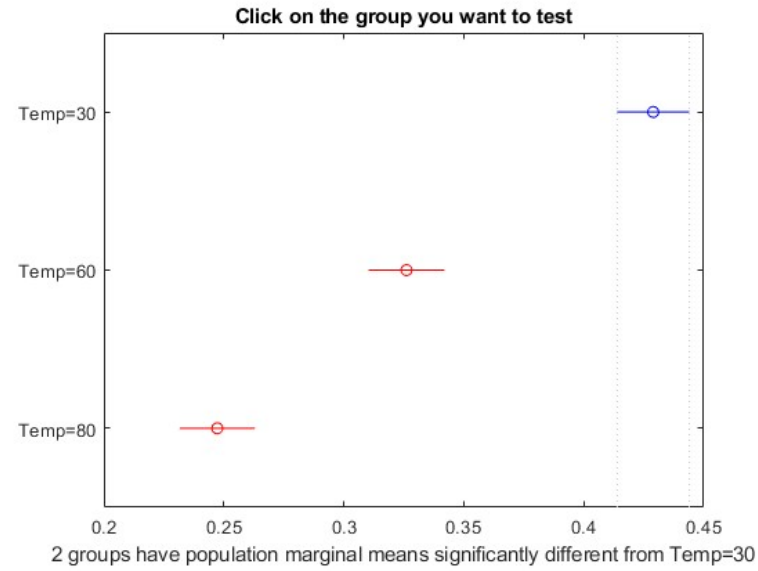

Figure 35: Post-hoc for temperatures, all measurements.

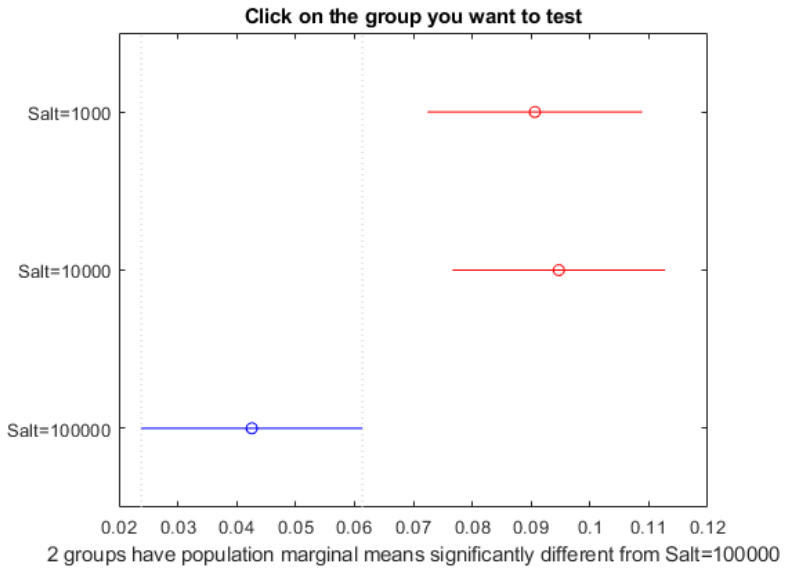

Figure 36: Post-hoc for OCP-Ecorr based on salt, not including salt levels 10 ppm and 100 ppm.

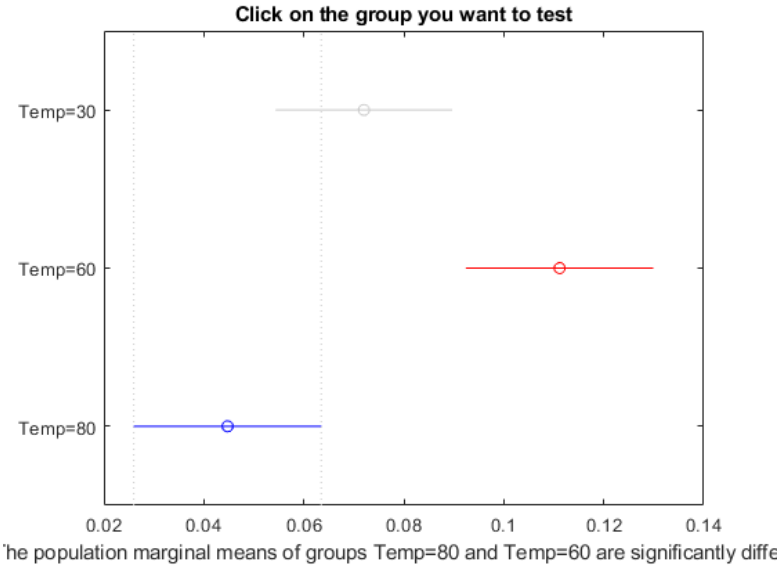

Figure 37: Post-hoc for OCP-Ecorr based on temperature, not including salt levels 10 ppm and 100 ppm.

A2 Surface roughness measurement from ALICONA

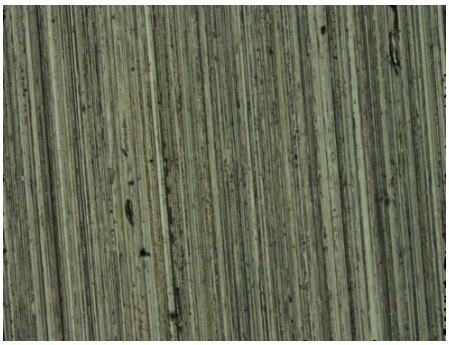

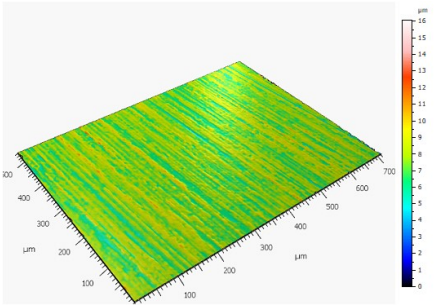

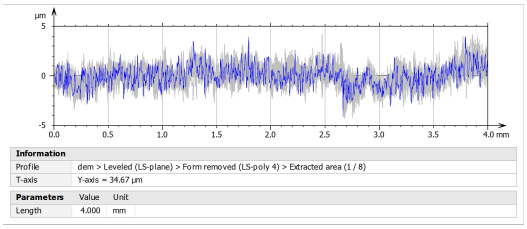

Information	
Profile	dem > Leveled (LS-plane) > Form removed (LS-poly 4) > Extracted area (1 / 8)
T-axis	Y-axis = 34.67 µm

Parameters	Value	Unit
Length	4.000	mm

		Context	Mean	Std dev	Min	Max
ISO 21920 - Roughness (S-L)						
F: None						
S-filter (λs): Gaussian, 2.5 µm						
L-filter (λc): Gaussian, 0.8 mm						
Evaluation length: All λc (5)						
Height parameters						
Rq	µm		0.8645	0.01403	0.8465	0.8881
Rsk			0.09092	0.06905	-0.01877	0.2095
Rku			3.186	0.1268	2.980	3.369
Rt	µm		6.560	0.3330	5.977	7.180
Rpt	µm	*Max of values on: All λc (5)*	3.208	0.4055	2.576	4.052
Rp	µm	*Average of values on: All λc (5)*	2.677	0.1680	2.342	2.865
Rvt	µm	*Max of values on: All λc (5)*	3.352	0.2724	2.996	3.855
Rv	µm	*Average of values on: All λc (5)*	2.601	0.1137	2.434	2.740
Rzmax	µm	*Max of values on: All λc (5)*	6.560	0.3330	5.977	7.180
Rz	µm	*Average of values on: All λc (5)*	5.278	0.1526	5.082	5.505
Ra	µm		0.6856	0.01432	0.6612	0.7094

Figure 38: Surface roughness measurements from ALICONA Optical Microscope.

A3 SOP for Sören

The objective of the following section is to provide a SOP for measurements and testing using the corrosion testing machine (Sören). Adjust as necessary to suit different parameters. This SOP does not

include how to run measurements at temperatures above 80 °C.

Sample preparation

Samples are cut and grinded from a long rod of metal. In the list below the procedures and for sample preparation is described.

- **Primary cutting:** The rod is placed and fastened in MACHINE NAME. Adjust the stopper, start the machine and let it fall down on the sample. Measure the sample length and adjust the stopper as necessary. Collect the samples, rinse of the coolant solution and dry using paper.
- **Pre-grinding:** To level out the surface and sharp edges grind the samples with a file. Fasten the sample and grind away from yourself. The surface does not have to be totally even, but eliminate sharp edges as to not rip och cause unnecessary damage to the grinding paper used in next step.
- **Grinding:** Using the grinder in the sample prep room, place samples in the specific holder (depicted in method section of this report). If not all the slots are filled, place them as evenly in the holder as possible. The machine has several programmes and settings, however for SS 316L and similar alloys manual preparation for 10-15s at a time yields good results. Use gloves as to not contaminate the grinding paper and sample surfaces. Attach the sample holder to the machine, lower the holder down and press start. After 10-15s stop, remove the holder and inspect the samples. Please refer to figure 11 for an example of sample after grinding using 220 SiC. Change sides of the samples that are polished enough and adjust positions of samples to be as even as possible if you remove ready samples. Increase the level of SiC-paper or use Piano, depending on desired surface roughness and surface finish. A starting point can be 220 SiC. However in ASTM standard G61 [31] and similar standards, grinding to 600 SiC is recommended.
- **Second cutting:** The second cutting is performed in the cutting machine in the sample prep room. Place the sample in the holder and fasten it. Use a cutting sheet suitable for the hardness of the alloy/metal, for SS 316L the sheet 30A15 is a good option. These can be found in the drawers below the machine. Fasten the plate and with sample in place adjust the position of the plate towards the sample. Press the forward with caution, if the plate touches any component or the sample it will break. Adjust the settings, however the settings provided in the routine 30A15 and 16mm track (depending on where you position the sample) is good. Adjust the speed when the cutting is ongoing to speed up the cutting, however be mindful and do not increase so that the pressure on the sheet does not pass to far into the orange and not the red-zone. After the cutting is finished, wash each sample in ethanol and place on its side on a clean surface. Remove the blade used and wipe the floor of the machine.
- **Ultrasonic cleaning:**Place the samples into clean beaker using a tweezer. Pour Ethanol (80wt%) so that it covers the samples. Pour water into the ultrasonic bath so that it reaches the operating line. Adjust and fasten the beaker so that it is well immersed in the water. Clean samples ultrasonically for approximately 5 minutes.
- **Packaging:** Dry in air after ultrasonic cleaning, on cleanroom-cloth. Cut up cloths to wrap samples in, place in plastic bag, assign a number to the sample and note in document which date it is packaged. Allow for oxidation for at least 7 days, the samples should be oxidized approximately the same amount of days.

Measurement using the corrosion testing machine (Sören)

- **Assemble test chamber:** First insert the O-ring into the chamber using a tweezer. Handle sample using gloves, wash with either ethanol or water to remove any particles on the sample. Place the sample in the holder, push it down and when possible put the screw in and screw the sample into position. Fasten the screw. Screw the electrodes into place, fasten the test chamber into its' position in Sören, tighten the screws around the test chamber. Place plastic container below the test chamber to catch potential spillage.
- **Solution preparation:** Weigh components with the scale in the same room as the corrosion testing machine. Mix using the magnetic stirrer or by hand in plastic container.
- **Using Nova + Autolab PGSTAT:**
- Start the software. From the main menu select previous methods and select the one you want. Check if the method is the one you have used before, check starting potentials and cutoff current. Start the measurement when the temperature is reached.
- Sometimes the computer does not recognize the Autolab-instrument. This can be solved by checking if the computer has underwent any updates, and retracting these. However, the problem can remain and the easiest could be to simply swap computer.
- **Measurement:**
- Select the temperature. Flow rate and pour the solution in. Press on main-switch, then the pump, heating and external cooler. Notice if everything looks fine. Let the temperature reach the set temperature and start the measurement in NOVA. The OCP-measurement should be ”alive” and not follow any repeated pattern. If this is not the case restart the Autolab-unit and computer.
- When the measurement is finished turn of heating and cooling, empty the machine by pumping the liquid out. Allow some liquid to stay in the tank and empty the last by using the ventil on the side. Close it and fill the tank with clean water and pump it through, repeating the procedure with emptying the last liquid in the side vessel, as to not damage the pump.

Cleaning

Cleaning after each measurement and CIP is described in section 3 of this report.

- The routine consists of four subsequent steps with the first being a rinse of approximately 4l water at room temperature. After this NaOH (1wt%) is circulated in the system at (50 °C for 60 minutes. The system is then rinsed with water again followed by HNO3 (1wt%) circulating in the system for 40 minutes, at (50 °C. The system is after this rinsed with water again and the acid is to be disposed in suitable storage. At the time of writing this report it's in the chemical locker in chemical safe flasks. To transport the acid from the lab to the room with Sören use the same bottle and close it.

A few good sentiments for operating the corrosion testing machine/Sören

- Restart computer and Autolab in between each measurement - this most of the time guarantees that the desk computer wont unexpectedly shut of - and or that the Autolab measurements is botched, as described in [10].

- Cooling takes a while which means that if you want to do a lot of measurements in a day - do low temp first if possible. Similar sentiments could be said about salt content - start low and increase during a day, to facilitate for accurate and good measurements. This might not be according to the DOE however it could allow for efficiency and the measurements do require some time.
- CIP should be done regularly, especially when the electrolyte is turbid - as you might not be able to see changes in color or ”clearness” by contamination.
- Rinse a lot in between experiments - increasing the frequency of the pump could make for more efficient cleaning but make sure to decrease it again to choosen frequency before next experiment.
- Biggest tip: use the water tap on the wall as it is faster.